DESTRESS

Demonstration of soft stimulation treatments of geothermal reservoirs

Deliverable D6.3: Technical performance monitoring and control

WP 6 Intelligent tools controlling performance and environment

Authors: Jan Henninges[1], Bob Paap[2]

[1] GFZ German Research Centre for Geosciences, Potsdam, Germany

[2] TNO, Applied Geosciences, Utrecht, Netherlands

Lead Beneficiary	GFZ
Type	☑ R - report, document etc. ☐ OTHER - software, technical diagram etc. ☐ DEM - demonstrator, pilot etc. ☐ E - ethics ☐ DEC - website, patent filing etc.
Status	☐ Draft ☐ WP manager accepted ☑ Project coordinator accepted
Dissemination level	☑ PU - Public ☐ CO - Confidential: only for members of the consortium
Contributors	☑ 1-GFZ ☐ 5-GES ☐ 9-GTL ☐ 13-SNU ☐ 2-ENB ☑ 6-TNO ☐ 10-UoS ☐ 14-KIC ☐ 3-ESG ☐ 7-ETH ☐ 11-TUD ☐ 15-ECW ☐ 4-UoG ☐ 8-GTN ☐ 12-NEX ☐ 16-WES
Creation date	20.02.2020
Last change	28.02.2020
Version	2.8
Due date	29.02.2020
Submission date	28.02.2020

This project has received funding from the European Union's Horizon 2020 research and innovation programme under grant agreement No 691728

Imprint

Project Lead GFZ German Research Centre for Geosciences
Telegrafenberg
14473 Potsdam (Germany)
www.gfz-potsdam.de/en/home/

Project Coordinator Prof. Ernst Huenges
huenges@gfz-potsdam.de
+49 (0)331/288-1440

Project Manager Dr. Justyna Ellis
ellis@gfz-potsdam.de
+49 (0)331/288-1526

Project Website www.destress-h2020.ch

Liability claim

DESTRESS is co-funded by

National Research Foundation of Korea (NRF)
Korea Institute for Advancement of Technology (KIAT)
Swiss State Secretariat for Education, Research and Innovation (SERI)

Table of contents

LIST OF TABLES

1 Introduction

The DESTRESS project is aimed at creating EGS (Enhanced Geothermal Systems) reservoirs with sufficient permeability, fracture orientation and spacing for economic use of underground heat. The main focus is on stimulation treatments with minimized environmental hazard ("soft stimulation"), in order to enhance the hydraulic performance of reservoirs in different geological settings. In the framework of this study, guidelines and tools for monitoring and well-test analysis in order to assess the technical performance of stimulation treatments have been developed. As a first step, generic monitoring design approaches and criteria have been defined, which were then updated using information from the soft stimulation treatments performed at the demonstation sites in the course of the project. The use of novel techniques, like distributed acoustic sensing (DAS), for improved monitoring of soft stimulation methods has been investigated. Environmental monitoring, especially including seismic hazard and safety, has been treated separately in Task 6.4 (see Grigoli et al. 2019).

2 Monitoring design approaches and criteria

The demonstration sites of DESTRESS included Pohang and Geldinganes, where soft cyclic stimulation has been tested, as well as Soultz-sous-Forêts, where a chemical stimulation treatment has been applied. In the following, the individual sites, the stimulations and the technical performance monitoring applied are briefly outlined, followed by an overview of tools and methods for technical performance assessment.

2.1 Pohang

The Pohang EGS project site is located in the SE part of the Korean peninsula, north of the city of Pohang. The project was launched in December 2010 by a consortium of industry partners (including the site owner and operator Nexgeo) and Korean research institutes. The target geothermal reservoir is fractured granodiorite basement rock, which is accessed by two wells PX-1 (4362 m depth, deviated with 22° inclination) and PX-2 (4348 m depth, vertical), with open hole sections of 313 m and 140 m, respectively, at the bottom.

Within the context of DESTRESS, a cyclic soft stimulation (CSS) treatment was performed in the PX-1 well in August 2017. The stimulation design, monitoring, and analysis of the hydraulic and seismic data was mainly carried out within Task 5.4 (Zimmermann et al. 2020). During a one-week period, a total volume of 1756 m^3 of fluid was injected in cycles with high-rate and low-rate injection between 1-10 l/s, reaching a maximum wellhead pressure of 22.8 MPa (Hofmann et al. 2019).

The monitoring of the stimulation treatment included recording of hydraulic parameters such as surface flow rates and wellhead pressures (see Table 2), as well as geochemical monitoring in order to investigate fluid-rock interactions (Westaway and Burnside 2019; Burnside et al. 2019). For monitoring of the hydraulic performance of the reservoir, the harmonic pulse testing (HPT) method was applied, which involved cyclic variation of the injection rate during stimulation (Fokker et al. 2018; Salina Borello et al. 2019). The productivity determined from these pulse tests is similar to the results obtained from conventional well test analysis.

Individual elements of the seismic monitoring network are listed in Table 3. It included a temporary seismic array within a radius of 7 km around the site, consisting of 5 surface stations, 8 shallow (up to

120 m depth) and one deep (2380 m) borehole stations, as well as a 17-level geophone chain, which was placed in the adjacent PX-2 well at 1350-1510 m depth (Hofmann et al. 2019).

While only two of the induced seismic events were strong enough to be recorded by a sufficient number of the surface and shallow borehole stations for hypocentre localization (Bethmann et al. 2019), the recordings of the downhole geophone chain enabled to detect 52 microseismic events in total (Hofmann et al. 2019). The localization is nevertheless partially ambiguous, because of registration in one single well only. The locations nevertheless overlap with the seismic cloud derived for an earlier stimulation of this well derived in the study of Bethmann et al. (2019).

On November 15, 2017, a MW 5.5 earthquake occurred close to the Pohang EGS site (Grigoli et al. 2018), after another stimulation had been performed by the operator Nexgeo in the PX-2 well in September 2017. Hydraulic stimulation at the Pohang site has been suspended thereafter.

2.2 Geldinganes

Following the first treatment at Pohang, further experiments on cyclic soft stimulation within DESTRESS have been performed the Geldinganes site in Iceland.

Geldinganes, an uninhabited peninsula within the city limits of Reykjavik, is characterized by an exceptionally high geothermal gradient of up to 400 °C/km, and a gabbro body at depth was identified as the potential heat source and target reservoir. The RV-43 well has been drilled in 2001 as a production well to be connected to the district heating system of the city of Reykjavik. It has a measured depth of 1832 m, including a 1130 m long open hole section with a deviation of up to 38°. As the necessary flow rates for economic heat production could not be achieved, its hydraulic performance should be improved by hydraulic stimulation. The site is owned and operated by Reykjavik Energy (Orkuveita Reykjavíkur, OR).

Within the context of DESTRESS, a cyclic soft stimulation treatment with multi-stage injection was performed in the RV-43 well in October 2019. The stimulation design and planning of the monitoring program was mainly carried out within Task 5.4 (Zimmermann et al. 2020). The stimulation design included cyclic injection with progressive flow rate changes with multi-stage injection using a straddle packer (Hofmann et al. 2020). During a 17-day period a total volume of approx. 20.000 m³ was injected into three individual stimulation intervals (Zimmermann et al. 2020).

Pre-stimulation logs included a camera inspection, caliper logs, acoustic borehole televiewer, and a neutron-neutron log. These logs were primarily recorded for planning of the stimulation treatment, i.e. identification of suitable intervals for setting the packers and localization of fracture zones as potential stimulation targets (Hofmann et al. 2020). Baseline temperature logs have been recorded to assess the initial temperature conditions before stimulation.

Hydraulic monitoring during the stimulation treatment included recording of the surface flow rates and fluid volumes (Zimmermann et al. 2020). Pressure was record both at the wellhead and downhole, i.e. above, below and between the packers using memory tools. Temperature logging performed between the individual stimulation treatments enabled to identify downhole injection zones, based on comparison with the pre-stimulation baseline logs, and operational issues such as casing leakages.

The design of the microseismic real-time monitoring network, seismic risk assessment, and development of a site-specific advanced traffic light system was mainly performed within Task 6.4 (Broccardo et al. 2019). Individual elements of the seismic monitoring network are listed in Table 3. It included temporary stations within a radius of 5 km around the site, consisting of 16 surface stations, 2 shallow borehole stations (25 and 122 m depth), as well as a 17-level geophone chain, which was placed at 1040-1200 m depth in the well R-42, at a distance of approx. 2.5 km from the injection well (Hofmann et al. 2019).

The detailed analysis of the recorded data, including hydraulic, seismic, and chemical monitoring is currently ongoing.

2.3 Soultz-sous-Forêts

The Soultz pilot EGS site is located in northern Alsace, France. The geothermal reservoir is formed by deep seated fractured granites of the crystalline basement of the Upper Rhine Graben. Five boreholes have been drilled to depths of 3.6 to 5 km (Genter et al. 2010), and several hydraulic and chemical stimulations have been carried out over time in order to improve the hydraulic performance of the reservoir. Since 2000, the site is owned by GEIE (European Economic Interest Group), a consortium of industrial companies, and operated by ÉS-Géothermie. A binary power plant producing 1.7 MW of electricity is in operation, and currently the well GPK2 is used as a producer and GPK3 and GPK4 as injectors.

In the framework of the DESTRESS project, the impact of a soft chemical stimulation treatment on injectivity during long term circulation is investigated. Within Task 4.3, a chemical stimulation treatment with low flow rate and localized acid injection in GPK4 well using a coiled tubing unit has been performed in December 2019 (Hehn et al. 2020). The main flush consisted of 2 x 50 m^3 of different acid mixtures, aimed to dissolve carbonates and silicate minerals (clays, quartz) sealing the natural fractures of the reservoir. The stimulation was performed at normal operating conditions, and injection was only shut-in for 5 hours to allow for chemical reaction of the treatment fluid and the formation close to the borehole.

Pre-stimulation well logs have been recorded in GPK4 in January 2018 in order to characterize the state of the well (well integrity) and planning of the chemical stimulation treatment (Vidal et al. 2018). These included flowmeter, caliper, acoustic borehole imager, and cement bond logs. Based on these logs, the main injection zones and intervals with borehole integrity problems (casing break, zones with bad cementation and deformed casing) could be identified. Two fracture zones in the open hole section and a leakage zone within the cemented part of the casing were selected as stimulation targets. It was decided to use a coiled tubing unit for selective fluid placement during the chemical stimulation, avoiding zones with poor borehole integrity.

Both hydraulic and chemical monitoring is part of the long-term monitoring at Soultz and was also performed during the chemical stimulation of GPK4 (Hehn et al. 2020). The evolution of injectivity is determined by measuring the wellhead pressure and flow rate at surface. Chemical monitoring of the geothermal brine produced and reinjected into the wells includes measurements of electrical conductivity, pH, major element concentrations, and gas composition. The primary focus of the chemical monitoring is to control and reduce scaling and corrosion processes in the surface installations.

Induced seismicity at the Soultz site is continuously monitored with a network consisting of eight surface stations within a radius of approx. 5 km from the site (Maurer et al. 2020). This network records the seismicity in real time during power plant operation, and was also used to for monitoring of seismicity during the chemical stimulation treatment. Two seismic events were detected during the stimulation phase, which were similar to the baseline microseismic activity at the site (Hehn et al. 2020). There was no evidence that these events were directly related to the stimulation treatment, and therefore it is not possible to delineate the extent of the stimulated rock volume using seismicity in this case.

2.4 Overview of tools and methods for technical performance assessment

Table 1: Technical performance assessment parameters.

Assessment parameter	**Input information**	**Measurand[a]**	**POH**	**GEL**	**SOU**
Energy output	Flowrate, quality (phase composition), and temperature of produced fluid	1.1, 1.2	(n.a.)	(n.a.)	Yes
Productivity/injectivity of well	At surface	1.1, 1.3	Yes	Yes	Yes
Location and size of stimulation intervals	Downhole	2.2.1, 2.3.1, 2.3.2	No	Yes	(BL)
Productivity/injectivity of individual reservoir/stimulation intervals		2.1.1, 2.2.1,	No	No	(BL)
Leakage detection (borehole integrity)		2.2.1, 2.3.1, 2.3.2	No	Yes	(BL)
Extent of induced fractures/stimulated rock volume	Location of induced seismic events during stimulation	1.4	Yes	Yes[b]	No[c]
Structural integrity of borehole casing and annular cementation, zonal isolation	Borehole integrity measurements	2.2.2, 2.2.3	(BL)	(BL)	(BL)

POH, GEL, SOU refers to the Pohang, Geldinganes, and Soultz demonstration sites, respectively (see Sections 2.1, 2.2, and 2.3) a) see Table 2. b) seismicity cloud detected, final evaluation ongoing. c) no seismicity related to stimulation observed. (BL): only baseline measurements available.

Table 2: Listing of measurement parameters, tools and methods.

Measu-rand	Measurement parameters	Sensors, tools and methods	POH	GEL	SOU
1.	**Surface monitoring**				
1.1.	Flowrate, quality (phase composition)	Flow meter	2 -	2 -	1 – 4 -
1.2.	Fluid temperature	Temperature sensor	-	-	4
1.3.	Fluid pressure	Pressure sensor	2	2	1 – 4
1.4.	Velocity/acceleration of ground motion	Seismometer array, microseismic monitoring (at surface, in shallow and/or deep boreholes, see Table 3)	1, 2, 4	1, 2, 4	1-4
2.	**Downhole monitoring**				
2.1.	***Point sensors***				
2.1.1.	Reservoir pressure	Pressure sensor	-	2	-
2.2.	***Electric wireline logging***				
2.2.1.	Profiles of pressure, temperature, velocity, density of produced/injected fluid over reservoir interval	Production logging tool, e.g. spinner flow meter with gradiomanometer	 - 1 - -	 - 1, 2 - -	 1 1 1 1
2.2.2.	Morphology/diameter of inner surface of borehole completion	Multi-finger caliper acoustic borehole scanner	1 1	1 1	1 1
2.2.3.	Sonic amplitudes/bond index, acoustic impedance of annular fill	Cement-bond log (CBL-VDL) acoustic borehole scanner	1 1	1 -	1 1
2.3.	***Fiber-optic sensing***				
2.3.1.	Repeated well temperature profiles	DTS (Distributed Temperature Sensing)	-	-	-
2.3.2.	Repeated profiles of dynamic strain changes or vibration along well	DAS (Distributed Acoustic Sensing)	-	-	-

POH, GEL, SOU refers to the Pohang, Geldinganes, and Soultz demonstration sites, respectively (see Sections 2.1, 2.2, and 2.3). Numbers refer to timing of monitoring campaigns (see listing below).

Timing of monitoring campaigns:

1. before treatment (base line)
2. during treatment (control of stimulation process)
3. after treatment (assess efficiency, e.g. fold of increase of productivity/injectivity, relative to base line measurement before treatment)
4. long-term monitoring during operation (sustainability of stimulation effect)
5. on demand, e.g. in case of unexpected developments (e.g. changes in productivity/injectivity) or technical problems (e.g. suspected leakages)

Table 3: Seismic monitoring networks deployed during stimulation treatments at DESTRESS demo sites.

Station type	**Pohang**	**Geldinganes**	**Soultz**
surface	5	16	8
Borehole, shallow	8 (82-125 m)	2 (25, 122 m)	-
Borehole, deep	1 (2380 m)	-	-
Borehole, geophone chain	17-level, 10m spacing, 1350-1510 m depth	17-level, 10m spacing, 1040-1200 m depth	-
Station radius (km)	7	5	5

3 Distributed acoustic sensing for borehole monitoring

Several aspects for the use of fiber-optic distributed acoustic sensing (DAS) for design of improved well monitoring procedures, in particular using vertical seismic profiling (VSP), have been investigated. In the following, brief summaries of the individual studies are given and the detailed descriptions are contained in the appendix.

3.1 DAS response modeling

Simulation of DAS data is important to assure the capability of DAS systems for technical performance monitoring in the Destress setting. Existing state-of-the-art seismic modelling software (SPECFEM) has been used and modified. Real field DAS VSP-data were acquired in cooperation with GFZ at the GFZ aquifer thermal energy storage exploration well Gt BChb 1/2015 in Berlin-Charlottenburg in September 2017, and has been used to compare and validate the simulation results. The model used is capable of simulating DAS data that closely resemble the real field data acquired at this site. An overview of the transfer functions that affect DAS acquisition footprint for different field settings has been developed. This can serve as a basis for future simulations of DAS measurements of thermal, hydraulic and chemical stimulation in order to assess the capability of DAS to detect the expected changes in the processes and properties of these stimulations.

More detailed descriptions of the DAS transfer functions, the numerical simulations and the results of the field experiment are contained in Appendix 1.

3.2 DAS-VSP case study Groß Schönebeck

The performance of the DAS method for vertical seismic profiling at an EGS site has been evaluated by analysis of an DAS-VSP dataset acquired at the Groß Schönebeck site. This is an EGS-site in a sedimentary environment, where cyclic multi-stage stimulation has been applied. In February 2017, a mini 3D DAS-VSP survey with 61 source points, and DAS registration in two wells up to ~4300 m depth, has been performed. Details of the data acquisition, seismic data processing and imaging results are contained in the paper by Henninges et al. (2019), which is contained in Appendix 2.

Key results of this study are as follows:

- Standard VSP products, like interval velocities, corridor stacks, and 3D-VSP images, can be generated with significantly reduced operational effort and cost compared to conventional sensors.

- Specific DAS recording characteristics, like directional sensitivity and lower signal-to-noise ratio, have to be considered during survey planning.
- Wireline cable deployment is especially relevant for deep geothermal wells, as installation of permanent cables is difficult/expensive due to well construction and completion (liner, packers, etc.).
- Suitable equipment/fiber-optic wireline cable is not readily available from service companies yet.
- Deployment: influence of cable tension on mechanical coupling and signal quality.
- Seismic data processing: a specific type of "ringing" noise has been observed, which can successfully be suppressed using suitable filtering methods.

3.3 DAS-VSP feasibility study Soultz

The feasibility of imaging steeply dipping fractures and faults in the basement at the Soultz site using DAS- VSP measurements has been investigated (see Appendix 3). Data from three previous VSP surveys recorded at Soultz site with conventional 3C borehole geophones are available.

Key results of the study are:

- Important structures can be detected using VSP, including main injection zones GPK4 determined from Jan. 2018 pre-stimulation well logs (casing leaks at approx. 4380 and 4700 m depth, see Vidal et al. (2018)).
- Recorded data contains significant information in vertical component, interpreted as p-s reflections from steeply dipping faults. This is of advantage for acquisition using DAS, where primarily the vertical component parallel to the cable/borehole axis is recorded.

4 Summary and conclusions

In the framework of this study, guidelines and tools for monitoring and well-test analysis in order to assess the technical performance of soft stimulation treatments have been developed. Parameters for assessment of the technical performance of a soft stimulation treatment have been defined, and an overview of measurement parameters, tools and methods is given, integrating experiences from the field experiments performed at the three demonstation sites Pohang, Geldinganes and Soultz.

The most relevant parameter for assessment of the overall performance of a geothermal well is the energy output, which is determined by the flowrate and temperature of the produced fluid. The hydraulic performance of a geothermal well is expressed by the injectivity or productivity index, which is commonly determined from the flowrate and the differential pressure at surface.

For monitoring of the hydraulic performance of the reservoir, harmonic pulse testing (HPT) is a promising new method. The productivity determined from HPT is similar to the results obtained from conventional well test analysis. As an advantage, HPT can be can be applied during production or injection, without requiring a shut-in of the well.

The extent of induced fractures and the stimulated rock volume can be delineated based on the locations of induced seismic events. For proper localization, the geometry and the sensitivity of the seismic network it is important. During the design, the local noise conditions should be considered. As an example, seismic stations located in surface outcrops of mudstones with high attenuation of seismic waves proved to be problematic at Pohang, and more stations in shallow boreholes reaching into underlying tuffs would have been preferable.

For multi-stage stimulation treatments, usually a more extensive downhole monitoring program is required than for open hole stimulations. Before stimulation, a more detailed characterization of the borehole and formation for selection of suitable stimulation intervals is necessary. During stimulation, downhole monitoring serves to ensure proper function of individual stimulation stages. Later on during operation, it is desirable to observe possible changes in in- or outflow behavior, or success of measures for reservoir management, e.g. in order to avoid thermal breakthrough, by shut-in or activation of individual stages.

The use of advanced techniques, like distributed fiber-optic sensing methods, bears great potential for downhole monitoring of technical performance. The value of distributed temperature sensing (DTS) has already been recognized for monitoring of EGS operation (e.g. Henninges et al. 2012; Blöcher et al. 2016). Temperature logging is a rather simple and cost effective method to identify downhole injection and production zones, based on comparison with the pre-stimulation baseline logs, and operational issues such as casing leakages. The use of the novel distributed acoustic sensing (DAS) method for improved well monitoring procedures was positively evaluated within several studies presented here. Deployment using wireline cable is especially of interest for deep geothermal wells, as installation of permanent cables might be challenging for typical well construction and completion practices applied here (also see e.g. Geo-Energie Suisse 2017). Specific challenges with respect to DAS response, sensor deployment and data evaluation could be tackled successfully already, but individual details still need further investigation, due to differences compared to conventional sensors.

References

Bethmann F, Ollinger D, Tormann T (2019) Seismicity analysis with spatial or temporal relation to the deep geothermal project in Pohang during 2016/2017. DESTRESS report. Geo-Energie Suisse AG,

Blöcher G, Reinsch T, Henninges J, Milsch H, Regenspurg S, Kummerow J, Francke H, Kranz S, Saadat A, Zimmermann G, Huenges E (2016) Hydraulic history and current state of the deep geothermal reservoir Groß Schönebeck. Geothermics 63:27-43. doi:10.1016/j.geothermics.2015.07.008

Broccardo M, Mignan A, Grigoli F, Karvounis D, Rinaldi AP, Danciu L, Hofmann H, Milkereit C, Dahm T, Zimmermann G, Hjörleifsdóttir V, Wiemer S (2019) Induced seismicity risk analysis of the hydraulic stimulation of a geothermal well on Geldinganes, Iceland. Nat Hazards Earth Syst Sci Discuss 2019:1-39. doi:10.5194/nhess-2019-331

Burnside NM, Westaway R, Banks D, Zimmermann G, Hofmann H, Boyce AJ (2019) Rapid water-rock interactions evidenced by hydrochemical evolution of flowback fluid during hydraulic stimulation of a deep geothermal borehole in granodiorite: Pohang, Korea. Appl Geochem 111:104445. doi:10.1016/j.apgeochem.2019.104445

Fokker PA, Salina Borello E, Verga F, Viberti D (2018) Harmonic pulse testing for well performance monitoring. J Pet Sci Eng 162:446-459. doi:10.1016/j.petrol.2017.12.053

Genter A, Evans K, Cuenot N, Fritsch D, Sanjuan B (2010) Contribution of the exploration of deep crystalline fractured reservoir of Soultz to the knowledge of enhanced geothermal systems (EGS). Comptes Rendus - Geoscience 342 (7-8):502-516. doi:10.1016/j.crte.2010.01.006

Geo-Energie Suisse (2017) D5.1: Description of Individual Completion Elements Required to Segment EGS Reservoir Section. DESTRESS project. Geo-Energie Suisse, Zürich

Grigoli F, Cesca S, Rinaldi AP, Manconi A, López-Comino JA, Clinton JF, Westaway R, Cauzzi C, Dahm T, Wiemer S (2018) The November 2017 Mw 5.5 Pohang earthquake: A possible case of induced seismicity in South Korea. Science. doi:10.1126/science.aat2010

Grigoli F, Wiemer S, Wassing V, Genter A (2019) Deliverable D6.4: Environmental performance monitoring for validation and control. DESTRESS project. ETH Zürich,

Hehn R, Cuenot N, Mouchot J, Maurer V, Genter A, Seibel O, Peterschmitt A, Imbs B, Reinsch T, Huenges E (2020) Deliverable D4.3 (M42), Reservoir performance in terms of sustainability. Application to the geothermal well GPK-4, Soultz-sous-Forêts. Destress project. ES-Géothermie (ESG), Stasbourg

Henninges J, Brandt W, Erbas K, Moeck I, Saadat A, Reinsch T, Zimmermann G (2012) Downhole monitoring during hydraulic experiments at the In-situ Geothermal Lab Groß Schönebeck. Proceedings, 37th Workshop on Geothermal Reservoir Engineering, Stanford, USA (CD-ROM):51-56

Henninges J, Martuganova E, Stiller M, Norden B, Bauer K, Krawczyk CM, Huenges E (2019) Exploration and Monitoring with Distributed Acoustic Sensing at the EGS Site Groß Schönebeck. In: Proceedings, European Geothermal Congress 2019. European Geothermal Energy Council, Bruxelles,

Hofmann H, Zimmermann G, Farkas M, Huenges E, Zang A, Leonhardt M, Kwiatek G, Martinez-Garzon P, Bohnhoff M, Min K-B, Fokker P, Westaway R, Bethmann F, Meier P, Yoon KS, Choi JW, Lee TJ, Kim KY (2019) First field application of cyclic soft stimulation at the Pohang Enhanced Geothermal System site in Korea. Geophys J Int 217 (2):926-949. doi:10.1093/gji/ggz058

Hofmann H, Zimmermann G, Zang A, Aldaz S, Cesca S, Heimann S, Mikulla S, Milkereit C, Dahm T, Huenges E, Hjörleifsdóttir V, Snæbjörnsdóttir SO, Aradóttir ES, Ásgeirsdóttir RS, Ágústsson K, Magnússon R, Stefánsson SA, Flovenz Ó, Mignan A, Broccardo M, Rinaldi AP, Scarabello L, Karvounis D, Grigoli F, Wiemer S, Hólmgeirsson S (2020) Hydraulic Stimulation Design for Well RV-43 on Geldinganes, Iceland. In: Proceedings World Geothermal Congress 2020, Reykjavik, Iceland. International Geothermal Association, pp 1-15

Maurer V, Gaucher E, Grunberg M, Koepke R, Pestourie R, Cuenot N (2020) Seismicity induced during the development of the Rittershoffen geothermal field, France. Geothermal Energy 8 (1):5. doi:10.1186/s40517-020-0155-2

Salina Borello E, Fokker PA, Viberti D, Verga F, Hofmann H, Meier P, Min KB, Yoon K, Zimmermann G (2019) Harmonic Pulse Testing for Well Monitoring: Application to a Fractured Geothermal Reservoir. Water Resour Res 55 (6):4727-4744. doi:10.1029/2018WR024029

Vidal J, Mouchot J, Cuenot N, Hehn R, Lucas Y, Schäfer G (2018) MS30, Second report on reservoir performance in terms of sustainability. Destress project. ES-Géothermie (ESG), Stasbourg

Westaway R, Burnside NM (2019) Fault "corrosion" by fluid injection: A potential cause of the November 2017 MW 5.5 Korean Earthquake. Geofluids 2019. doi:10.1155/2019/1280721

Zimmermann G, Hofmann H, et al. (2020) Deliverable D5.2: Demonstration of reservoir treatment (cyclic stimulation) and long-term performance of energy production. DESTRESS project. GFZ German Research Centre for Geosciences,

Appendix

Appendix 1: Distributed Acoustic Sensing (DAS) performance monitoring for validation and control (TNO report May 2018 DESTRESS WP6.3)

Distributed Acoustic Sensing (DAS) performance monitoring for validation and control

Arie Verdel, Bob Paap, and Stefan Carpentier

Introduction

This brief report describes the TNO-contribution to WP6, task 6.3, of EU-H2020 project DESTRESS.

DESTRESS is aimed at creating EGS (Enhanced Geothermal Systems) reservoirs with sufficient permeability, fracture orientation and spacing for economic use of underground heat by demonstration of soft stimulation treatments of geothermal reservoirs. Work package WP6 of DESTRESS, entitled “Intelligent tools controlling performance and environment” is aimed at developing workflows and tools that enable decision makers to deploy the demonstrated stimulation strategies on other settings proactively by reduction of uncertainty in energy production estimates, and through adoption of rigorous monitoring and control loops, safeguarding environmental and technical performance, and sustainability. Task 6.3, forming part of WP6, to which GFZ, TNO and TUD contribute, specifically concern the development of workflows for technical performance monitoring for validation and control. The TNO-contribution to task 6.3 deals with the investigation of the usefulness of employment of Distributed Acoustic Sensing (DAS) technology in Vertical Seismic Profiling (VSP) acquisition. The list of specific technical objectives is presented in the section hereunder.

Objectives

- Attain overview of transfer functions relevant in DAS-VSP seismic acquisition. Specific focus on TNO interrogator with Berlin DAS-VSP demo as test case.
- Synthetic approach to address the performance of DAS for vertical seismic profiling (VSP): Use initial modeling approach for DAS-VSP measurements. This can serve as a basis for future research to address different acquisition geometries and detectability of different types of stimulation techniques by DAS-VSP measurement.
- Establish detectability of ground motions in the borehole in the presence of the identified transfer functions of DAS.
- Discuss implications of DAS transfer functions for detectability of changes in reservoir properties and processes due to well stimulation.

Background

Destress WP 6.3 involves the technical performance monitoring for validation and control of well stimulation operations. Many facets of well stimulation need to be controlled, such as temperature, flow, flow paths, injected volumes, proppant volumes, precipitation and other processes. Geophysical monitoring techniques suitable for performance monitoring include seismic, Electro-Magnetic (EM), gravity and optical methods. These are capable of imaging and monitoring changes in the processes and properties of stimulation. Of these methods, the seismic method has the highest resolving power.

The most important borehole seismic and well-logging surveys aiming at imaging near-well reservoir structure around the borehole are Vertical Seismic Profiling (VSP), Sonic Logging and Acoustic Imaging Logging. These surveys all require seismic sensors in the borehole clamped to the casing or measurements taken in open hole. During production or stimulation of the well however, the casing and cement will always be in place, and when VSP is considered, seismic recordings have to take place in noisy conditions in a cased well (unless you have a separate monitoring well nearby). This is not optimal and will hamper the seismic data quality because of 1) high noise levels due to stimulation operations and 2) poor coupling of the sensors to the reservoir because of the presence of the casing. The repeatability of the seismic survey in time lapse applications will suffer even more from these issues.

Distributed Acoustic Sensing (DAS)

A new seismic sensor technology can counter most of these problems: Distributed Acoustic Sensing (DAS), also known as distributed vibration sensing, is a relatively new method for recording VSP data using a fibre optic cable as the sensor [1-7]. The signal obtained from such systems is a distributed measurement over a length of cable defined as the gauge length.
Gauge length selection appears to be one of the most important acquisition parameters for a distributed vibration sensing survey [8]. If the gauge length is too small, then the signal-to-noise ratio will be too low. If the gauge length is too large, resolution will be reduced and the shape of the wavelet will be distorted. The optimum gauge length is a function of the propagation velocity and frequencies of the seismic waves being measured. In a VSP recording in general, particularly the propagation velocities vary considerably over the recording depth interval of the survey, and therefore different gauge lengths are recommended for achieving optimum data quality.

Using optical interferometry, strain within the fibre is measured down to micrometer level and up to 1000 Hz. The gauge length, approximately corresponding with spatial sensor-recording interval in conventional point sensor recording , is in the order of 1-10 meter. A total fibre optic length of 10 km is available for recording and thus up to +- 10000 channels can be effectively used. Recording bandwidth is 1- 1000 Hz which is considered broadband in seismic acquisition. Currently, quite some conventional seismic acquisition systems exist with similar specs, but what really sets DAS apart is where and when it can record. The measuring string of DAS is merely a fibre optic cable, whereas conventional geophone systems have bulky sensors, cables and boxes. WiFi solutions exist, but are not suitable around metal casing. Most important: DAS fibres can access locations and under conditions that are out of reach for conventional geophones. A DAS fibre can be mounted outside the casing, in the cement or even outside the cement for direct contact with the reservoir. The fibre can withstand high overpressures and temperatures, up to 100 bar and 250° C. The fibre is also much less susceptible to noise.

A DAS acquisition system is currently being built and tested at TNO, however it is not yet operational for use in assigned Destress wells. But before any acquisition will take place, simulation of the DAS system must be done to assure the capability of the system for technical performance monitoring in the Destress setting.

DAS performance monitoring for Vertical Seismic Profiling (VSP)

In collaboration with GFZ (Potsdam) as well as with TNO Acoustics and Sonar, knowledge on acquisition and analysis of fibre optic DAS-VSP data was shared. The focus was specifically set on estimating the influence on expected signal-to-noise ratio (S/N) of DAS-VSP measurements in a geothermal reservoir due to typical VSP/borehole-specific acquisition constraints such as the presence of casing and cement. By identifying the key elements of a chain of DAS transfer functions of interest to VSP data acquisition, see Fig. 1, the influence of these factors on VSP signal quality can be analysed.

The actual identification of the DAS acquisition transfer functions was done in a joint effort with GFZ. As shown in Fig. 1, we can distinguish four categories of transfer functions:

Category 1. Geological formation-specific: transfer function 6.
Category 2. Borehole-completion/condition-specific: transfer function 5.
Category 3. DAS-cable-specific: transfer functions 2,3, and 4.
Category 4. DAS acquisition system ("interrogator" electronics) -specific: transfer function 1.

As indicated in Fig. 1., category 3 is being analysed by GFZ. This is work in progress and the completion date of it is as yet unknown. Category 1 concerns the spatial distribution of the subsurface medium properties, in particular seismic wave velocities and density, and can formally be regarded as a transfer function for wave propagation in a DAS-VSP, but is not DAS-specific and its analysis can therefore be absorbed in conventional seismic modelling and processing analysis. Furthermore, category 4 deals with acquisition system performance analysis of the TNO-built interrogator. Also, this category concerns ongoing work. For practical reasons, viz. given the timing and budget constraints for TNO in WP6.3., it was therefore decided to limit our investigation to categories 1. and 2.

<u>Can we neglect the influence of casing and cement (transfer function 5) on data of a VSP recorded with a DAS cable?</u>

A simple approach to address this question is a theoretical one: Fig. 2 shows the elementary wavelength-based analysis that is carried out in the following for P-waves (for S-waves a similar analysis can be performed): given the range of seismic frequencies of interest, and given the range of P-wave velocities in the subsurface area of interest, the resulting wavelength range for P-waves can be simply calculated (assuming an isotropic medium).

It can be safely concluded that these wavelengths measure at least two orders of magnitude larger than the realistic estimates for the cement and casing thicknesses, see Fig. 2. Wave scattering theory reveals that scattering objects with size much smaller than the wavelengths of interest can be neglected: the scattered energy is weak enough to be neglected in processing and analysis of the seismic data.

For near-vertical incidence of the P-wave (assuming a vertical well) or, more generally speaking, for near-along-borehole incidence of the P-wave, either transmitted or reflected, the apparent thicknesses, viz. the path lengths of the wave in cement and casing measured along the propagation direction, become larger with a factor 1/sin (alpha), with alpha being the angle between P-wave propagation direction and local borehole axis direction, see Fig. 2. These apparent thicknesses thus approach the smallest P-wavelength of interest only for angles alpha smaller than ~1 degree with the borehole axis. This corresponds in practice with the zero-offset VSP acquisition configuration and this configuration is not considered of interest for the time-lapse study of reservoir flow via well stimulation. In this analysis we neglect refraction due to velocity contrasts between formation, cement and casing (Snell's law), which we justify by the argument that the influence of the wave propagation on apparent thickness, viz. the factor 1/sin (alpha), is by far dominant as compared to the effect of refraction on apparent thickness.

From this we conclude that we can neglect the influence of casing and cement on data of a VSP recorded with a DAS cable as long as we do not include incoming wave directions very close to the borehole axis (say, within a few degrees).

This conclusion is confirmed by the shallow-well DAS-VSP field data recorded in an urban environment (Berlin) and discussed hereunder: fibre-optic strings were attached both inside and outside the casing- and cement layers. The DAS response recorded in both fibres were highly similar and could therefore be used for signal stacking.

This result can be further verified in more detail using field data by investigating wave propagation attenuation factors for the P-wave reflections of interest as function of depth by comparing the cement bond logging data in the same depth interval with the DAS-VSP reflection strength (measured in a single geological layer), see also the section hereunder. It is important to test this approach in future work.

The influence of geological formations on DAS-VSP data quality: transfer function 6

Transfer functions can be applied to synthetic DAS-VSP records obtained with 2D wave propagation software. Our developed modeling approach for DAS-VSP measurements serves as a basis for future research to address detectability of different types of stimulation techniques. Once effects of various types of thermal, hydraulic and chemical well stimulations are determined, they can be translated into estimated impedance effects, and used to address the detectability of time-lapse effects by synthetic DAS -VSP data.

Existing state-of-the-art spectral finite element seismic modelling software, SPECFEM2D [9], was used in our study as a basis for analysis of achievable signal quality in the VSP configuration. Figure 3 features a SPECFEM2D simulation which demonstrates, among other things, the influence of top-layer propagation velocity on the DAS-VSP response (surface-related multiple reflection and transmission strength is determined to a large extent by near-surface layer velocities) .

Comparing a modelled VSP-panel with the processed Berlin DAS-VSP data, see Fig. 5., we observe a striking correspondence, at least kinematically, for the down going wave system (the direct wave and its surface-related multiples, see Fig. 4). This is an encouraging result. As the upward travelling reflection data are one to two orders of magnitude smaller than the direct wave amplitudes, the demands on reflection data acquisition and processing are high. The feasibility analysis of detection of reflection amplitudes in the DAS-VSP is ongoing work.

The way forward

Apart from finalisation of DAS-VSP reflection amplitude analysis, future work will have to focus on extending the simulated, viz. modelled, DAS-VSP measurements with transfer function data such that the combined influence on the final processing result of DAS-VSP field data can be understood and thus interpreted. This scheme will need to represent realistic DAS acquisition imprints, transfer functions and other effects. With this modified software, time-lapse DAS measurements of thermal, hydraulic and chemical stimulation can be simulated in order to assess the capability of DAS to detect the expected changes in the processes and properties of these stimulations. One can think of changes that have an impedance effect such as temperature fronts, induced fracture networks, fluid pathways, proppant injection and such.

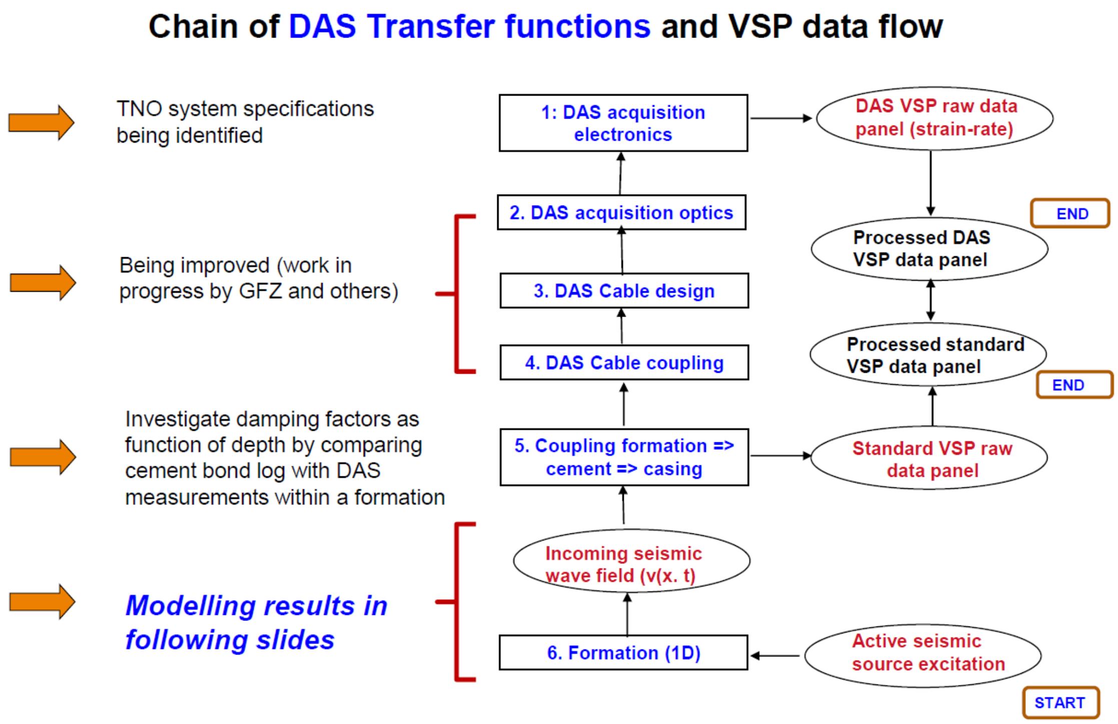

Fig. 1. DAS VSP data acquisition and -processing flow showing (in blue) key transfer functions (factors affecting VSP signal quality).

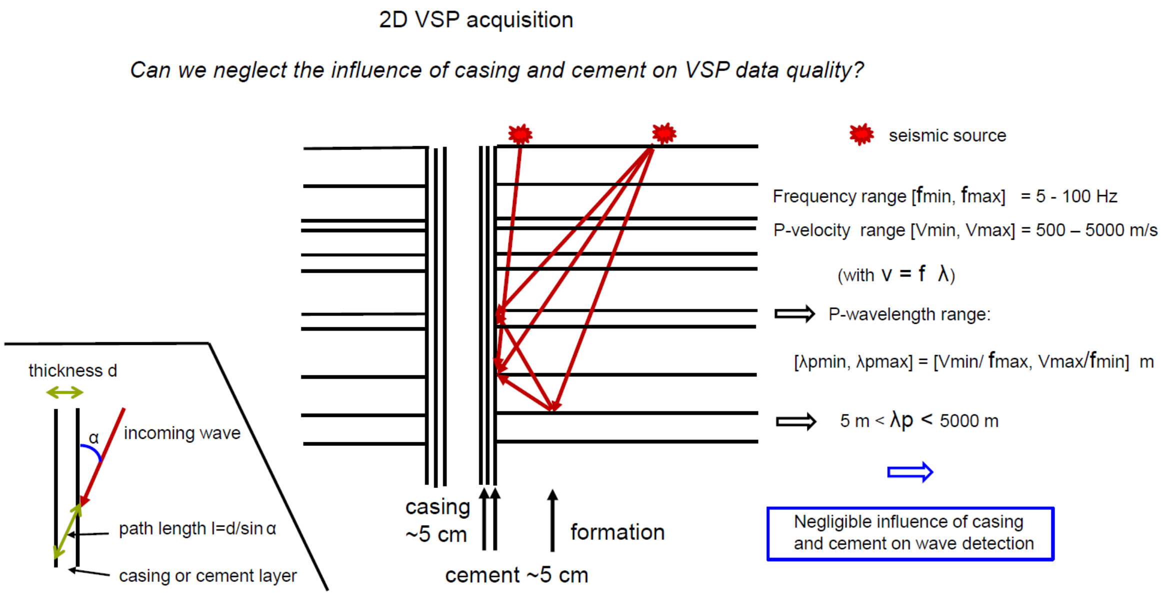

Fig. 2. 2D VSP acquisition layout, with 1D subsurface, showing typical ray paths (in red). For realistic seismic frequencies and P-wave velocities, the range of wavelengths of interest in VSP-recording exceeds the thicknesses of casing and cement to such an extent (two orders of magnitude) that the influence of those on VSP data quality can be neglected. Bottom left: relation between incoming wave direction and path length for layer with thickness d. Refraction is thereby neglected.

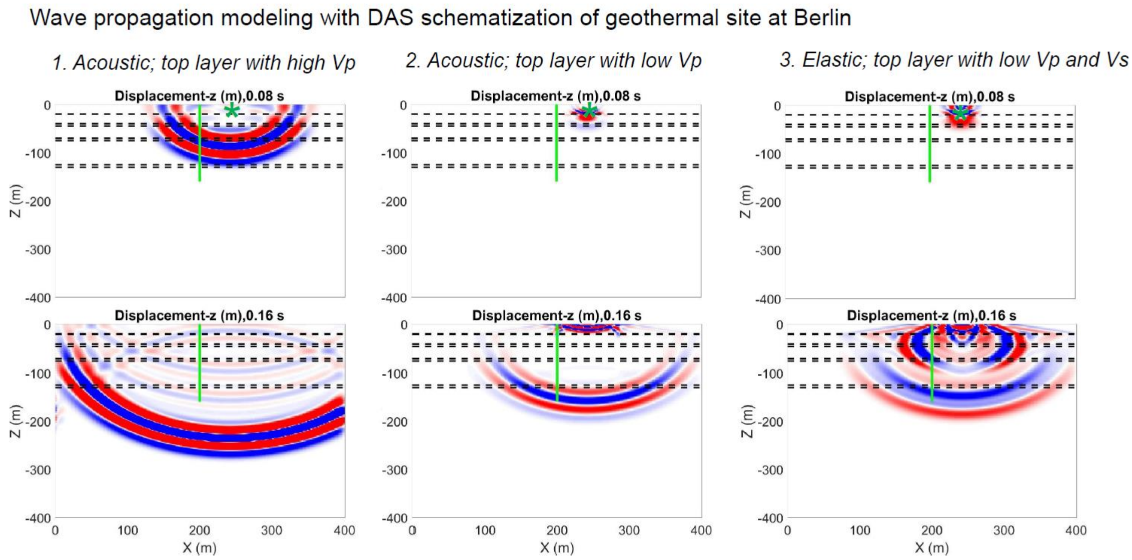

Fig. 3. Finite element (SPECFEM2D) acoustic and elastic wave propagation modelling examples of simulation of the Berlin DAS-VSP geometry. In '3. elastic' (on the right), attenuation is also included in the modeling. Note that the panels are scaled individually for display purposes implying that a quantitative comparison of amplitudes for the respective panels cannot be made. However, the overall amplitudes decrease from scenario 1 (left) to 3 (right).

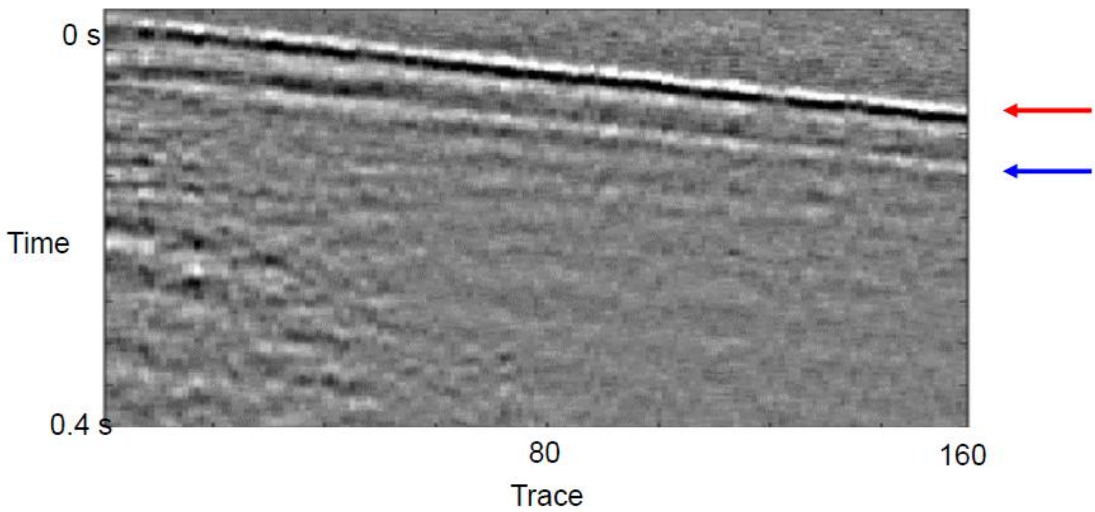

Fig. 4. Berlin DAS-VSP field data panel. Shot offset is 3 m. Recording depth is increasing in the rightward direction. Trace spacing is 1 m. Note the strong downward travelling direct wave (red arrow) and its highest order surface multiple (blue arrow).

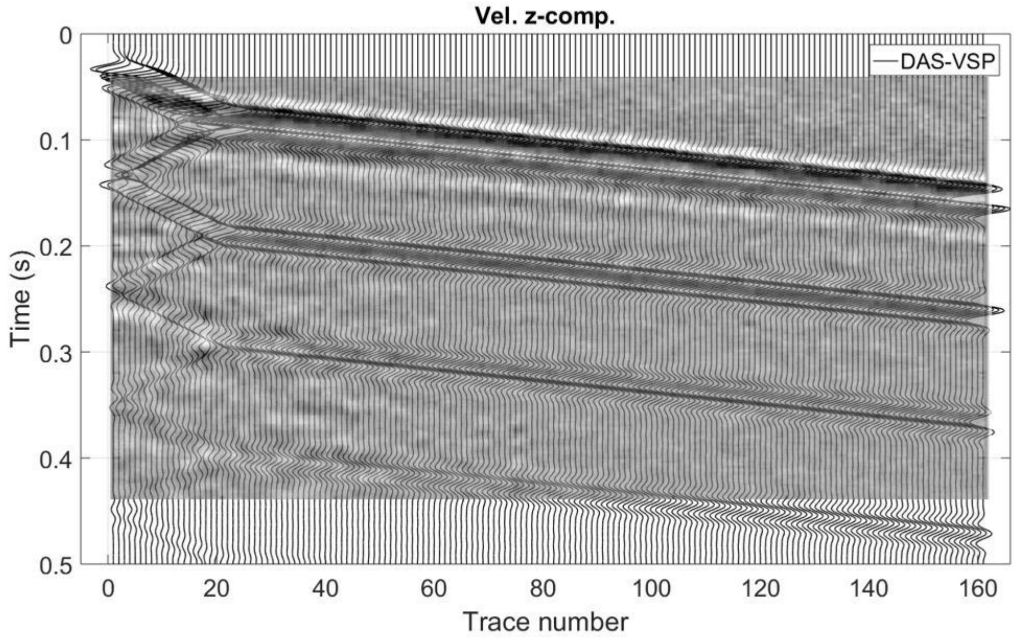

Fig. 5. Modelled DAS-VSP response (z-component of velocity) plotted as wiggle traces on top of DAS VSP field data panel. Shot offset is 3 m. Recording depth is increasing in the rightward direction (trace spacing 1 m). Note the striking correspondence between modelled and field data for the downward travelling wave system viz. the direct wave and related free surface multiples.

References

1. Lumens, P. G. E. [2014] Fibre-optic sensing for application in oil and gas wells, Technische Universiteit Eindhoven DOI: 10.6100/IR769555
2. Mateeva, A., Lopez, J., Potters, H., Mestayer, J., Cox, B., Kiyashchenko, D., Wills, P., Grandi, S., Hornman, K., Kuvshinov, B., Berlang, W., Yang, Z. and Detomo, R. [2014] Distributed acoustic sensing for reservoir monitoring with vertical seismic profiling. *Geophysical Prospecting*, **62**, 679-692.
3. Daley, T., Freifeld, B., Ajo-Franklin, J., Dou, S., Pevzner, R., Shulakova, V., Kashikar, S., Miller, D., Götz, J., Henninges, J. and Lüth, S. [2013] Field testing of fiber-optic distributed acoustic sensing (DAS) for subsurface seismic monitoring. *The Leading Edge*, **32**(6), 699-706.
4. Daley, T. M., D. E. Miller, K. Dodds, P. Cook, and B. M. Freifeld [2015] Field testing of modular borehole monitoring with simultaneous distributed acoustic sensing and geophone vertical seismic profiles at Citronelle, Alabama. *Geophysical Prospecting*, n/a, http://dx.doi.org/10.1111/1365-2478.12324.
5. Parker, T., Shatalin, S. and Farhadiroushan, M. [2014] Distributed Acoustic Sensing – a new tool for seismic applications. *First Break*, **32**, 61-69.
6. Götz J., Lüth S., Henninges J., Reinsch T. [2015] Using a fibre optic cable as Distributed Acoustic Sensor for Vertical Seismic Profiling at the Ketzin CO2 storage site. Conference Proceedings, 77rd EAGE Conference & Exhibition, Madrid, Spain (CD-ROM). doi:10.3997/2214-4609.201413363.
7. Correa, J., Van Zaanen, L., Tertyshnikov, K., Dean, T., Pevzner, R., Bona, A. [2017] DAS Versus Geophones: a Quantitative Comparison of a VSP Survey at a Dedicated Field Laboratory,

Proceedings, BGP10, Fourth EAGE Workshop on Borehole Geophysics 19-22 November 2017, Abu Dhabi, UAE.

8. Dean, T., Cuny, T. & Hartog, A.H. [2016] The effect of gauge length on axially incident P-waves measured using fibre optic distributed vibration sensing: *Geophysical Prospecting*, 65, 184-193.
9. Tromp, J., D. Komatitsch, and Q. Liu [2008] Spectral-element and adjoint methods in seismology. *Communications in Computational Physics*, 3(1):1–32.

Appendix 2: Exploration and Monitoring with Distributed Acoustic Sensing at the EGS Site Groß Schönebeck

Exploration and monitoring with distributed acoustic sensing at the EGS site Groß Schönebeck

Jan Henninges[1], Evgenia Martuganova[1], Manfred Stiller[1], Ben Norden[1], Klaus Bauer[1], Charlotte Krawczyk[1,2], and Ernst Huenges[1,2]

[1] GFZ German Research Centre for Geosciences

[2] Technical University of Berlin

janhen@gfz-potsdam.de, Telegrafenberg, 14473 Potsdam, Germany

Keywords: Geophysical exploration and monitoring, distributed acoustic sensing, fiber-optic sensing, Groß Schönebeck, enhanced geothermal system, stimulation.

ABSTRACT

Vertical seismic profiling has been performed at the Groß Schönebeck site in order to gain more detailed information on the structural setting and geometry of the geothermal reservoir. Data acquisition was performed using the novel method of distributed acoustic sensing, using hybrid wireline fiber-optic sensor cables deployed in two 4.3 km deep wells. During the four-day survey, data for 61 source positions was acquired. From the recorded data, accurate time-depth relationships, velocity and reflection profiles along the wells were derived. We show that structural elements near the boreholes can be imaged with high resolution, despite gaps in the data due to sparse coverage exist. The DAS method has enabled measurements at elevated temperatures up to 150 °C and has led to significant time and cost savings compared to deployment of a conventional geophone chain. Important new experiences for application of this non-standard method of acquisition have been gathered.

1. INTRODUCTION

The Groß Schönebeck site is located 40 km N of Berlin in the state of Brandenburg, Germany. It is a research platform that has been set up in order to test if production of geothermal energy from deep-seated reservoirs in the North German Basin is feasible. An enhanced geothermal system (EGS) has been created by hydraulic stimulation of low-permeability sedimentary and volcanic rocks of lower Permian (Rotliegend) age (Huenges et al. 2006; Zimmermann et al. 2010). For further development of the site, the implementation of a new stimulation concept and drilling of a new well have been proposed (Blöcher et al. 2015).

In order to gain more detailed information on the structural setting and geometry of the reservoir, a 3D seismic survey within an 8x8 km permit area has been carried out in February and March 2017 (Krawczyk et al. submitted). In addition, vertical seismic profiling (VSP) has been performed within the two 4.3 km deep research wells E GrSk3/90 and Gt GrSk4/05 existing at the site. The primary aims of the VSP survey were to establish precise time-depth and velocity profiles, and to image structural elements in the vicinity of the boreholes with higher resolution in three dimensions. A special challenge is imaging of structures within the reservoir interval of the Rotliegend at 4200 m depth, which is overlain by a 1400 m thick Zechstein salt complex.

The VSP measurement was performed using the novel method of distributed acoustic sensing (DAS). This method is based on optical time-domain reflectometry, and enables to register strain changes along optical sensor cables with high spatial and temporal resolution (Parker et al. 2014). Within recent years, a growing number of VSP surveys has been reported, where the DAS method has successfully been applied using sensor cables permanently installed behind casing or along tubing (e.g. Mestayer et al. 2011; Daley et al. 2013; Götz et al. 2018). In contrast to this, within this study the DAS data was acquired on wireline cables only temporarily deployed inside the wells, a method for which only very few experiences exist until now.

2. SURVEY DESIGN AND ACQUISITION

The target area was defined by the positions of the existing wells, the expected extent of the hydraulic fractures, and the trajectory of the proposed new well. It has a horizontal extent of approx. 700 x 500 m and a vertical thickness of approx. 300 m. A spiral pattern of 61 source points with offsets between 180 m and 2000 m from the wellheads was chosen, in order to achieve a good coverage of the target area and a uniform distribution of azimuths (Figure 1). Survey planning was based on well trajectories and geometry of the major geologic units (Moeck et al. 2009), taking into account DAS specific acquisition characteristics like directivity and signal-to-noise ratio. The source point positions were optimized based on ray tracing, using average acoustic properties of the major geologic units from a previous regional seismic survey (Bauer et al. 2010). The actual source point locations were then adjusted according to the conditions within the survey area, i.e. location of roads and agricultural areas, as well as required distances to sensible infrastructures like gas lines or buildings.

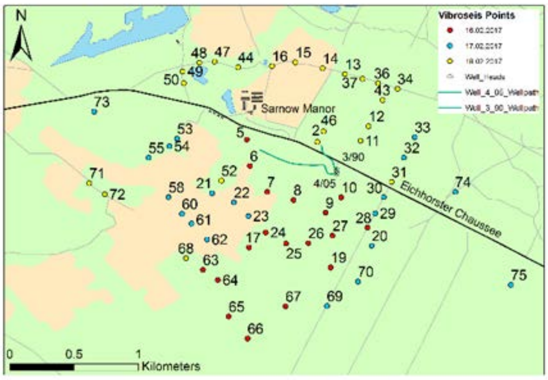

Figure 1: Survey area with VSP source point positions and borehole trajectories.

Field work was carried out within four days from Feb. 15-18, 2017. Energy excitation was performed with four Mertz M12 vibrator trucks simultaneously at each source position (45.100 lbs peak force). For acquisition of the DAS data in well E GrSk3/90 the GFZ hybrid borehole measurement system was used, which allows for deployment of fiber-optic sensors and electric downhole tools in parallel (Henninges et al. 2011). This well is near-vertical (maximum inclination 7.2°), and the fiber-optic data was acquired to a measured depth (MD) of 4256 m, which corresponds to a true vertical depth (TVD) of 4245.8 m below ground level. Within the well Gt GrSk 4/05, which is deviated up to 49° in the reservoir interval, a second wireline cable was deployed by Schlumberger (maximum DAS acquisition depth 4196 m MD / 4126.09 m TVD). Within this well additional measurements with a VSI (Versatile Seismic Imager) tool including a conventional three-component borehole seismometer were collected for comparison. DAS data was acquired using two Schlumberger hDVS (Heterodyne Distributed Vibration Sensing) units.

At the beginning a start-up test was carried out. Here suitable source and recording parameters were determined, including sweep frequencies, DAS gauge length and wireline cable tension. As a result, mainly a sweep with 10-112 Hz (linear) and 36 s duration was used during acquisition. For DAS data recording, a gauge length of 20 m was selected. This value was further adjusted for individual data sets during post-processing, based on the optimization procedure described by (Dean et al. 2017).

Within the following three days, acquisition was performed with a nominal number of 16 repeats for the 61 source positions distributed around the wells. The DAS measurements were recorded with a sampling rate of 2 ms and 5 m channel spacing across the entire length of the wells. Nevertheless, due to a technical problem during the second day of acquisition, only data for well GrSk3 could be recorded afterwards.

2.1 Basic seismic data processing

As one of the first processing steps, the DAS data recorded along the length of the sensor cables was correlated to well depths. Seismic pre-processing included stacking and correlation with the pilot sweep. The hDVS output strain data was then transformed to strain rate (time derivative), and further methods for conversion to geophone-equivalent data have been tested (Martuganova et al. submitted).

3. RESULTS

Shot gathers for a zero-offset position (VP 10) are displayed in Figure 2 and Figure 3. Over several intervals along the wells a specific noise with a zig-zag pattern can be recognized in the DAS data. Several approaches to reduce this ringing noise have been tested (Martuganova et al. submitted), e.g. using time-frequency domain (TFD) filtering, the result of which is displayed in Figures 2 and 3 for comparison.

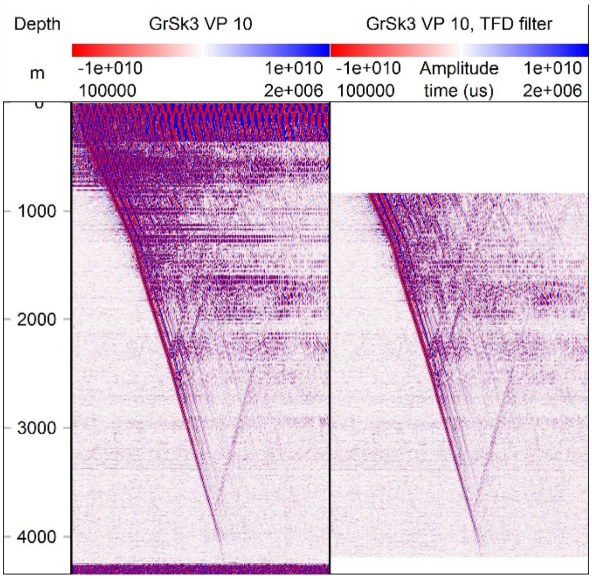

Figure 2: Zero-offset shot gathers for well GrSk3.

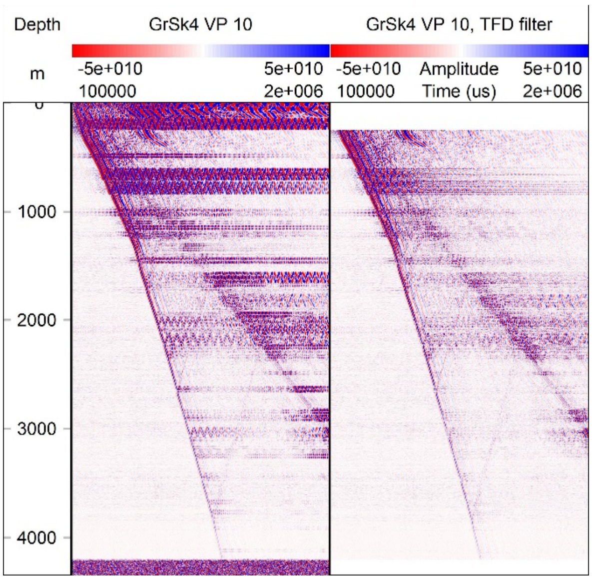

Figure 3: Zero-offset shot gathers for well GrSk4.

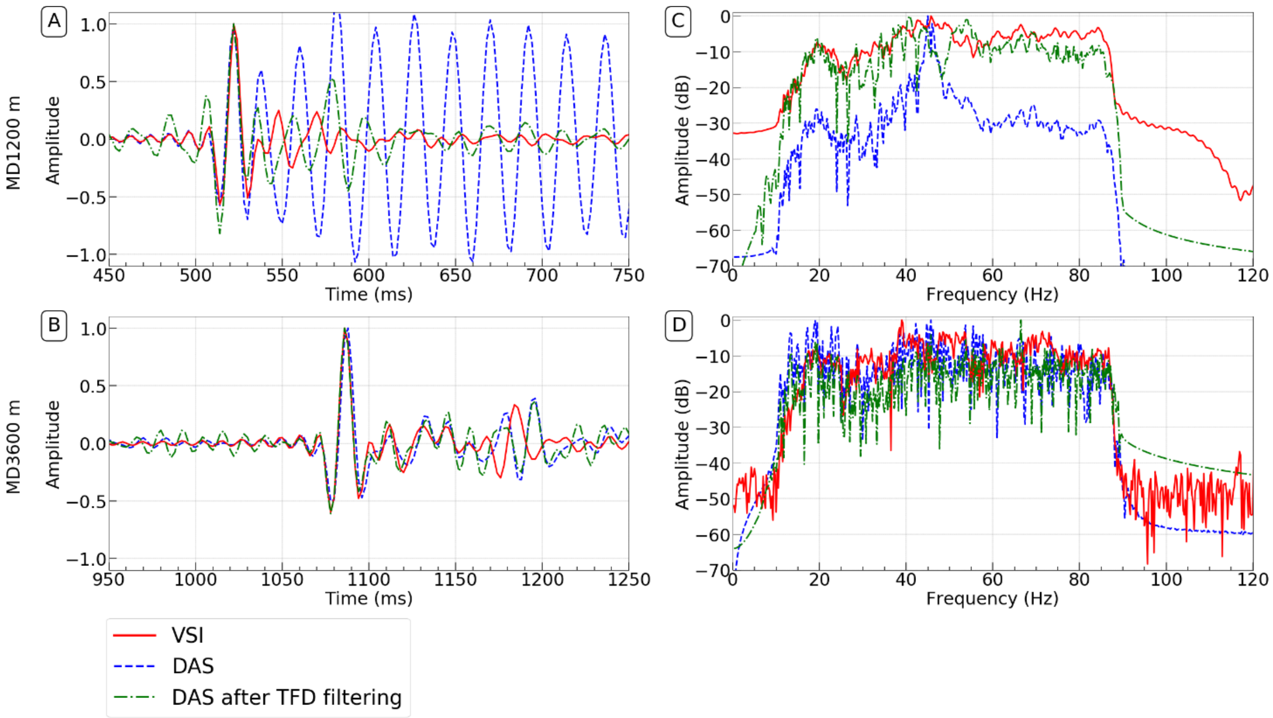

Figure 4: VSP traces and frequency spectra for VSI accelerometer and DAS strain-rate data recorded in well GrSk4 at 1200 m (A, C) and 3600 m (B, D) depth.

For well GrSk4, check shots at several depths were recorded with the VSI tool. A comparison between the vertical component of the VSI accelerometer data and the DAS data recorded at these depths is displayed in Figure 4. At 3600 m, the DAS strain-rate data shows very good agreement with the data from the accelerometer overall, which also applies to other depths recorded. At 1190 ms a temporary reversal of the polarity of the DAS signal compared to the accelerometer record is evident. At this time the signal is dominated by a strong reflection (see Fig. 3), originating from the base of the Zechstein interval.

The DAS trace for 1200 m depth is strongly influenced by the ringing noise described above, which is confined to a narrow frequency band between 40 and 50 Hz (Fig. 4c). The VSI tool data at this depth nevertheless shows a normal response, which suggests that the ringing noise in the DAS data is related to the different deployment methods of the acoustic receivers.

3.1 Zero-offset VSP processing

The arrival times of the direct down-going waves were picked in the zero-offset shot gathers. From these, time-depth relationships were established and interval velocities along the wells have been calculated (Figure 5). Variations within the VSP interval velocity profile show a good correlation to stratigraphy and the dominant lithologies. The calculated VSP interval velocities vary between about 2.8 and 5 km/s, and agree well to the compressional velocities of a sonic log previously recorded in the lower part of the well.

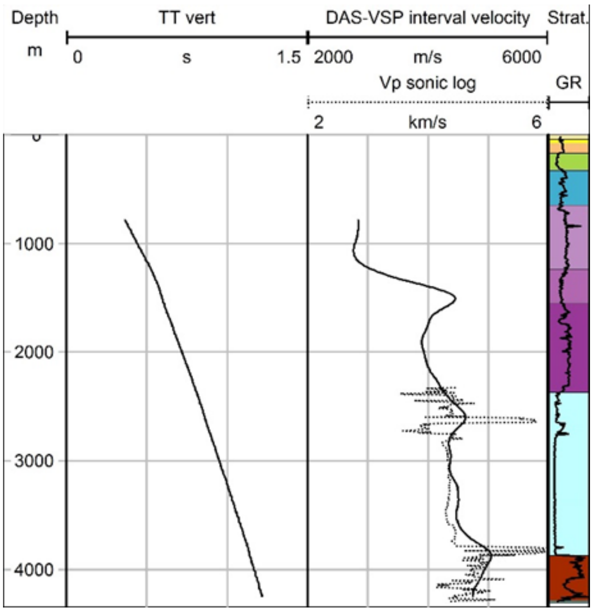

Figure 5: Vertical travel times (TT vert) and VSP interval velocities for well GrSk3. Stratigraphic units and a gamma-ray log (GR) are displayed in the track on the right.

Further processing steps included separation of up- and down-going wavefields, deconvolution, and transformation to two-way travel time. Afterwards vertical reflection profiles (corridor stacks) were generated from the separated upgoing wavefield data. A corridor stack for GrSk3 is displayed in Figure 6. The recorded reflections can be precisely assigned to logging data and lithological information from the wells using the time-depth relationships established before. The most prominent reflections occur near the top and the base of the Zechstein interval, and reflections within the Rotliegend reservoir interval are evident as well.

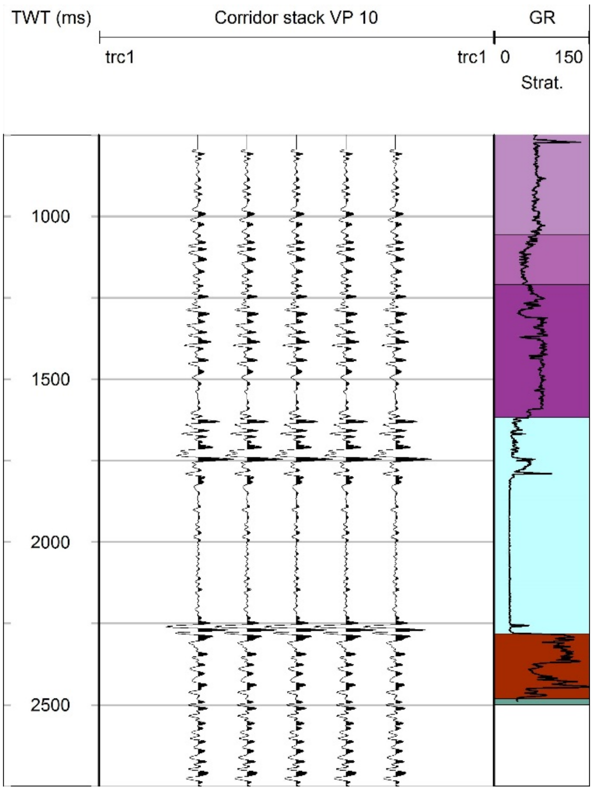

Figure 6: Corridor stack for well GrSk3 in two-way travel time (TWT). Right panel shows stratigraphic units and gamma-ray log (GR).

3.2 3D VSP imaging

As an input for 3D VSP imaging, the data from the other 60 offset positions recorded in well GrSk3 was processed in a similar way. The starting velocity model was based on previous information available, including well log data and a geological model based on vintage seismic data (Moeck et al., 2009), as well as post-stack time migration results of the 3D surface seismic data. The velocity model was then calibrated using the first-arrival travel times from the 61 VSP positions. The 3D VSP imaging was performed using a proprietary method based on beam-migration in combination with common depth-point mapping (VSProwess Ltd).

The generated seismic volume is displayed in Figure 7. It covers the target area around the wells which is imaged with high spatial resolution. As only data from one instead of two receiver wells could be used, zones with low coverage exist in the data volume. These low-fold zones were therefore blanked in order to exclude migration artefacts and avoid erroneous interpretations. The resulting data volume is therefore characterized by frequent gaps. Nevertheless important structural features can be identified, like an overall horizontal layering, different intervals with either parallel or divergent reflectors, and the absence of faults with larger vertical offsets.

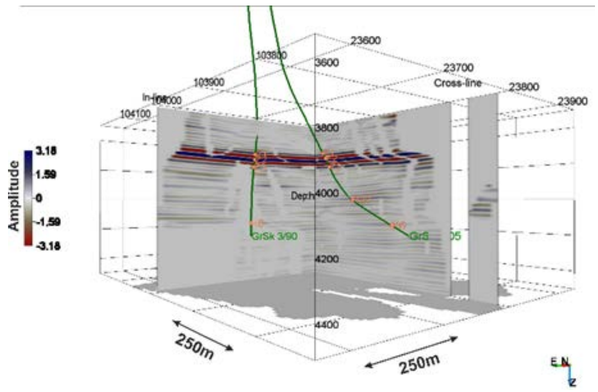

Figure 7: 3D VSP image, with vertical in-line and cross-line sections, well trajectories (green), and marker horizons (orange). Low-fold areas have been blanked (gray). Depths in meters below sea level (TVDSS).

4. CONCLUSIONS AND OUTLOOK

Based on this survey, important new experiences for DAS-VSP acquisition on wireline cable have been gathered. From the zero-offset data, accurate time-depth relationships and velocity profiles were derived. Integrated with other well data and geological information, these serve as input into the evaluation of the 3D surface seismic data set. We show that despite severe constraints during acquisition, structural elements near the boreholes can be imaged with high resolution using 3D-VSP processing. Further processing of the data is ongoing including processing of additional partial records available for well GrSk4, testing of different methods for noise suppression and wavefield separation, as well as other imaging techniques like Kirchhoff migration. The DAS method has enabled measurements at elevated temperatures up to 150 °C and has led to significant time and cost savings compared to deployment of a conventional geophone chain.

Acknowledgements

We acknowledge the good cooperation with the service companies Schlumberger and DMT GmbH & Co KG during data acquisition and processing of the zero-offset VSP data, as well as VSProwess Ltd during the 3D VSP imaging, and GGL Geophysik und Geotechnik Leipzig GmbH for survey planning. Jörg Schrötter, Christian Cunow, and Mathias Poser of GFZ supported the field work and acquisition of fiber-optic data. This project has been funded by the German Federal Ministry for Economic Affairs and Energy, grant no. 0324065, and the European Union's Horizon 2020 research and innovation programme under grant agreement no. 691728.

REFERENCES

Bauer K, Moeck I, Norden B, Schulze A, Weber M, Wirth H (2010) Tomographic P wave velocity and vertical velocity gradient structure across the geothermal site Groß Schönebeck (NE German Basin): Relationship to lithology, salt tectonics, and thermal regime. J Geophys Res 115 (B8):B08312. doi:10.1029/2009jb006895

Blöcher G, Cacace M, Reinsch T, Watanabe N (2015) Evaluation of three exploitation concepts for a deep geothermal system in the North German Basin. Comput Geosci 82:120-129. doi:10.1016/j.cageo.2015.06.005

Daley TM, Freifeld BM, Ajo-Franklin J, Dou S, Pevzner R, Shulakova V, Kashikar S, Miller DE, Goetz J, Henninges J, Lueth S (2013) Field testing of fiber-optic distributed acoustic sensing (DAS) for subsurface seismic monitoring. The Leading Edge 32:699-706. doi:10.1190/tle32060699.1

Dean T, Cuny T, Hartog AH (2017) The effect of gauge length on axially incident P-waves measured using fibre optic distributed vibration sensing. Geophys Prospect 65 (1):184–193. doi:10.1111/1365-2478.12419

Götz J, Lüth S, Henninges J, Reinsch T (2018) Vertical seismic profiling using a daisy-chained deployment of fibre-optic cables in four wells simultaneously – Case study at the Ketzin carbon dioxide storage site. Geophys Prospect 66:1201–1214. doi:10.1111/1365-2478.12638

Henninges J, Baumann G, Brandt W, Cunow C, Poser M, Schrötter J, Huenges E (2011) A novel hybrid wireline logging system for downhole monitoring of fluid injection and production in deep reservoirs. Conference Proceedings, 73rd EAGE Conference & Exhibition, Vienna, Austria (CD-ROM):C043

Huenges E, Trautwein U, Legarth B, Zimmermann G (2006) Fluid Pressure Variation in a Sedimentary Geothermal Reservoir in the North German Basin: Case Study Groß Schönebeck. In: Zang A, Stephansson O, Dresen G (eds) Rock Damage and Fluid Transport, Part II. Pageoph Topical Volumes. Birkhäuser Basel, pp 2141-2152. doi:10.1007/978-3-7643-8124-0_6

Krawczyk CM, Stiller M, Bauer K, Norden B, Henninges J, Ivanova A (submitted) 3-D seismic exploration across the deep geothermal research platform Groß Schönebeck north of Berlin/Germany. Geothermal Energy

Martuganova E, Henninges J, Stiller M, Bauer K, Norden B, Krawczyk C, Huenges E (submitted) DAS-VSP measurements using wireline logging cable at the Groß Schönebeck geothermal research site, NE German Basin. 81st EAGE Conference & Exhibition 2019, London, UK

Mestayer J, Cox B, Wills P, Kiyashchenko D, Lopez J, Costello M, Bourne S, Ugueto G, Lupton R, Solano G, Hill D, Lewis A (2011) Field trials of distributed acoustic sensing for geophysical monitoring. In: SEG Technical Program Expanded Abstracts 2011. Society of Exploration Geophysicists, pp 4253-4257. doi:10.1190/1.3628095

Moeck I, Schandelmeier H, Holl H-G (2009) The stress regime in a Rotliegend reservoir of the northeast German Basin. International Journal of Earth Sciences (Geol Rundschau) 98 (7):1643-1654

Parker T, Shatalin S, Farhadiroushan M (2014) Distributed Acoustic Sensing – a new tool for seismic applications. First Break 32 (2):61-69. doi:10.3997/1365-2397.2013034

Zimmermann G, Moeck I, Blöcher G (2010) Cyclic waterfrac stimulation to develop an Enhanced Geothermal System (EGS)—Conceptual design and experimental results. Geothermics 39:59–69

Appendix 3: Feasibility of DAS-VSP survey at Soultz to improve imaging of fault and fracture zones within the crystalline basement of the geothermal reservoir

Feasibility of DAS-VSP survey at Soultz to improve imaging of fault and fracture zones within the crystalline basement of the geothermal reservoir

E. Martuganova and J. Henninges

GFZ German Research Centre for Geosciences

18.07.2018

GFZ Helmholtz Centre Potsdam

HELMHOLTZ

Presentation outline:

- Introduction:The Soultz-sous-Forêts Enhanced Geothermal System (EGS)
- Overview of existing datasets:
  - Acquisition campaign 1988
  - Acquisition campaign 1993
  - Acquisition campaign 2007
- Optimizing the design of vertical seismic profiling (VSP)
- Suggestions for the planning of DAS VSP survey
- Methods for faults-fracture zones characterisation: tube-wave processing and analysis, seismic processing and imaging

GFZ Helmholtz Centre Potsdam

HELMHOLTZ

The Soultz-sous-Forêts Enhanced Geothermal System (EGS)

Mapping the geometry of permeable and non-permeable zones in crystalline rocks is fundamental for:

- natural fluid flows characterization ;
- evaluate the possibility of making artificial fluid circulations.

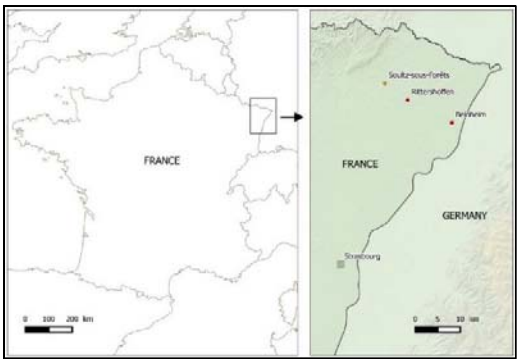

Baujard, C., et al. (2017).

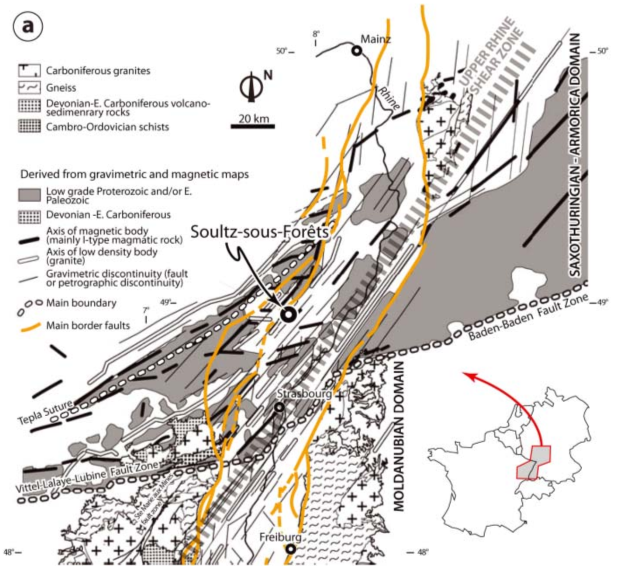

Place, J., et al. (2011).

Acquisition campaign 1988

(3C) receivers

- zero-offset VSP : 27 receiver positions, depth range 1250-2000m (30m spacing); 6 check shots at 100, 300, 500, 700, 900 and 1050m
- 3 offset VSPs: 17 receiver levels, depth range 1250-1730 m (30m spacing), offsets 500-900m.

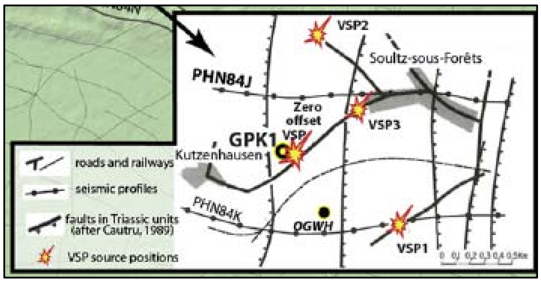

Location map of the zero offset and the three offset-VSPs acquired in 1988 (modified after (Beauce et al., 1991)).

Place, J., et al. (2010).

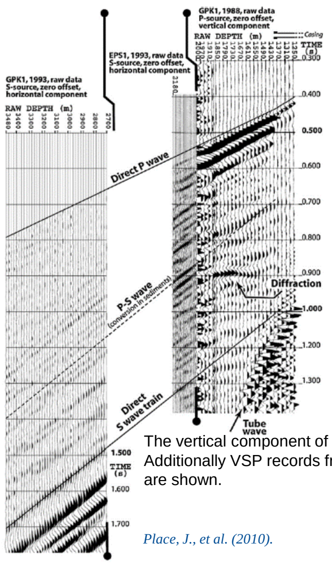

The vertical component of the zero offset VSP acquired in 1988. Additionally VSP records from the 1993 acquisition in GPK1 and EPS1 are shown.

Place, J., et al. (2010).

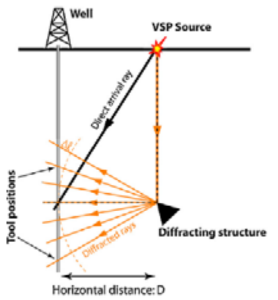

Sketch of the ray path recorded in a VSP survey when diffraction occurs

Acquisition campaign 1988

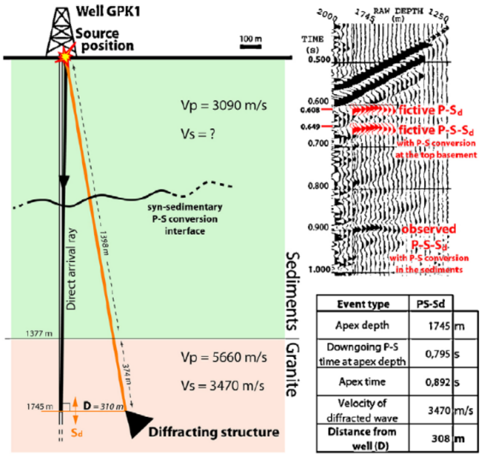

Event type	PS-Sd	
Apex depth	1745	m
Downgoing P-S time at apex depth	0,795	s
Apex time	0,892	s
Velocity of diffracted wave	3470	m/s
Distance from well (D)	308	m

Place, J., et al. (2010).

Diffracted propagation in a simplified model.

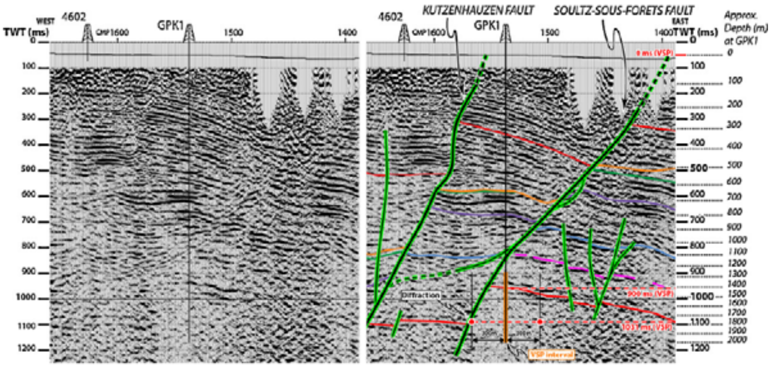

Place, J., et al. (2010).

PHN84J seismic reflection profile before and after interpretation in the Soultz-sous-Forets fault area. The diffraction could occur at the two red point locations.

GFZ Helmholtz Centre Potsdam

HELMHOLTZ

Acquisition campaign 1993

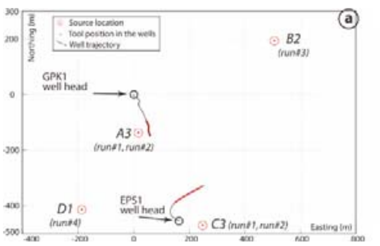

Position map of the *P*-seismic source position during the 1993 VSP survey and trajectory of the GPK1 and EPS1 wells

Place, J., et al. (2011).

- (3C) receivers
- A vertical vibrator was used to preferentially generate *P* waves
- 40 levels per VSP set (2700–3480 m with 20 m spacing in GPK1 and 1790–2180 m with 10 m spacing in EPS1).

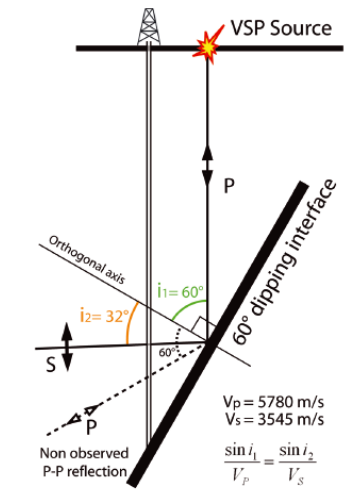

$$\frac{\sin i_1}{V_P} = \frac{\sin i_2}{V_S}$$

$$i_2 = \sin^{-1}\left(\frac{V_2}{V_1} \times \sin i_1\right) = \sin^{-1}\left(\frac{3545}{5780} \times \sin 60°\right) \approx 32°$$

Place, J., et al. (2011).

Seismic arrivals recorded :

- mainly in the vertical components ;
- observed at similar time–depth curves on several profiles .

They are interpreted as *P–S* reflections occurring on faults.

GFZ Helmholtz Centre Potsdam

HELMHOLTZ

Acquisition campaign 1993

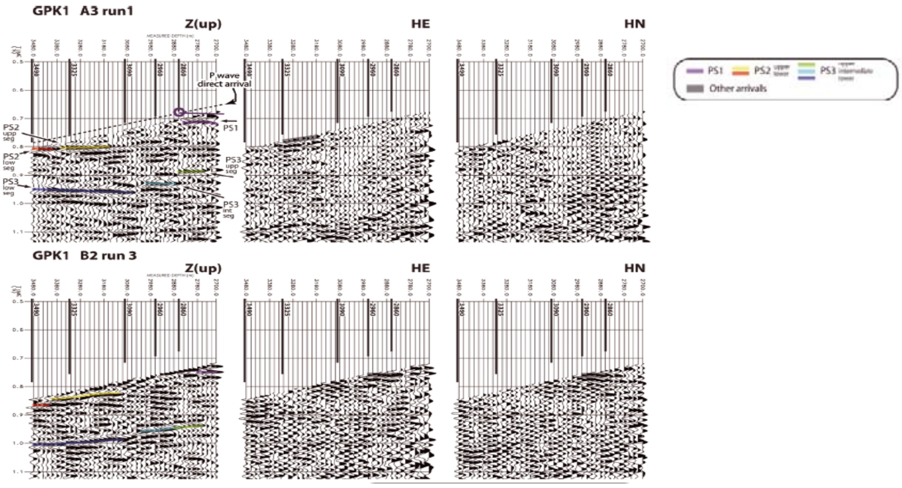

Three component signals of VSPs acquired at Soultz-sous-Forets in 1993 after isotropic processing HE and HN are, respectively, horizontal East and North components; *Z* is the vertical (up) component.

Place, J., et al. (2011).

GFZ
Helmholtz Centre
POTSDAM

HELMHOLTZ

Acquisition campaign 1993

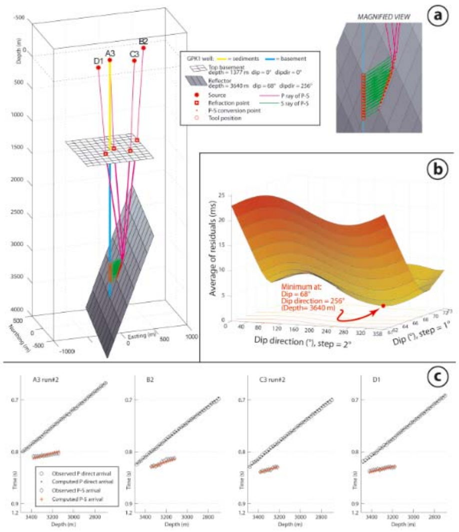

Place, J., et al. (2011).

Example of traveltime modelling applied to arrival PS2-upp-seg.

(a) 3-D plot showing the geometry of the velocity model and the ray paths.
(b) Residuals of modelling in the field of the investigated orientations.
(c) Observed and synthetic arrivals PS2-upp-seg, for the reflector position given in b (N256°E 68°).

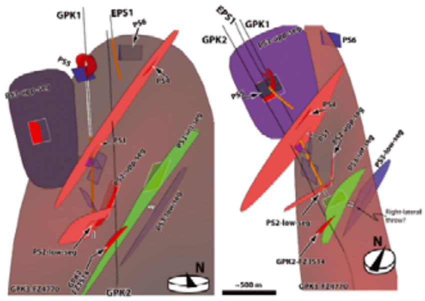

3-D views of the reflectors in the reservoir model built with gOcad.

Place, J., et al. (2011).

VSP Name	M.D. (m)	T.V.D. (m, below EPS1 well head)	Dip (°)	Dip Dir. (°)	Top (m, T.V.D. below GPK1 or ESP1 well head)	Bottom (m, T.V.D. below GPK1 or EPS1 well head)	Width (m)	Confidence
GPK1-PS1	2860	—	57	295	2700	2860	10	**
GPK1-2960	2960	—	51	045	2840	2960	1	*
GPK1-3090	3090	—	67	255	2845	3090	1	*
GPK1-3325 solution#1	3325	—	63	080	3100	3325	20	*
GPK1-3325 solution#2	3325	—	63	260	3100	3325	20	*
GPK1-PS2-low-seg	3490	—	52	324	3400	3490	10	***
GPK1-PS2-upp-seg	3640	—	68	256	3050	3420	30	***
GPK1-PS3-low-seg	4267	—	59	297	3150	3515	100	*
GPK1-PS3-int-seg	4384	—	63	329	2710	3050	170	**
GPK1-PS3-upp-seg	4362	—	68	150	2650	2910	180	**
EPS1-2070	2070	—	Domain		—	—	—	**
EPS1-2160	2160	—	Domain		—	—	—	**
EPS1-PS4	—	2496	59	297	1820	2090	20	**
EPS1-PS5	—	2655	49	150	2075	2240	60	*
EPS1-PS6 solution#1	—	3937	64	195	2030	2230	150	*
EPS1-PS6 solution#2	—	2650	55	325	2100	2325	150	*

List of reflectors detected by VSP, with orientations deduced from traveltime modelling.

GFZ
Helmholtz Centre
POTSDAM

HELMHOLTZ

Acquisition campaign 2007

Receivers:

- Recording with multi-component geophones
- Recording depth intervals along the well: GPK3 2000-4980 meters,GPK4 100-4980 meters

Source:

- 24 VPs, The multi-offset, multi-azimuth VSP, offsets 417 - 4967 meters
- Excitation: 2 vibrator vehicles, vibrating simultaneously with orthogonal sweeps, out of phase, frequency range 8-88Hz, duration period 16s, listening time 3 s.

Location VPs in the VSP 2007 campaign

Lavadera, P. L. (2013).

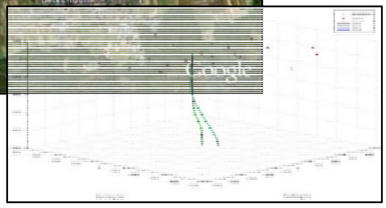

Location geophones (green points) in GPK3 well (black line) and GPK4 (blue line) for all shooting positions (red cross).

Lavadera, P. L. (2013).

GFZ Helmholtz Centre Potsdam

HELMHOLTZ

Acquisition campaign 2007

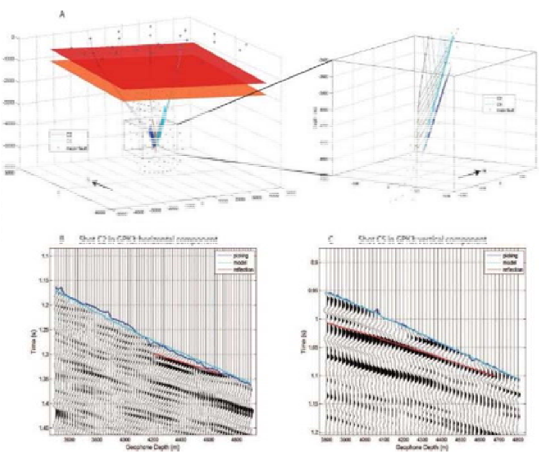

Modeling of the reflection on the major falt for both VPs C2 and C5 recorded in the well, b: VSP recorded on a horizontal component for the C2 c: VSP recorded on the vertical component of C5 shot.

Lavadera, P. L. (2013).

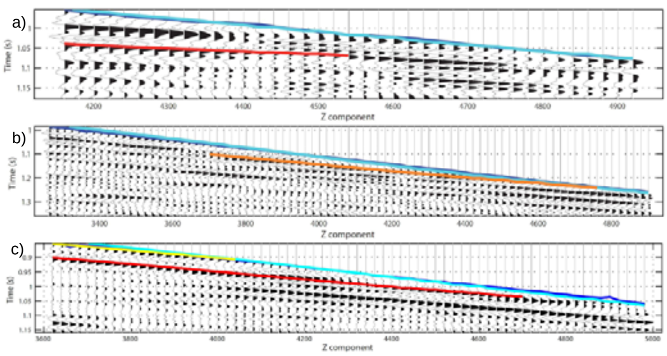

Modeled travel times for various modeled reflectors which correspond to reflected arrivals observed on the Z component of the geophones.

Lavadera, P. L. (2013).

GFZ Helmholtz Centre Potsdam

HELMHOLTZ

Acquisition campaign 2007

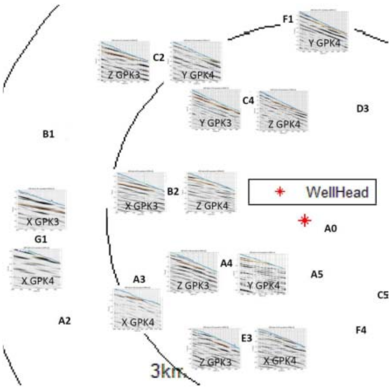

VSP datasets used for SIS3 structure imaging

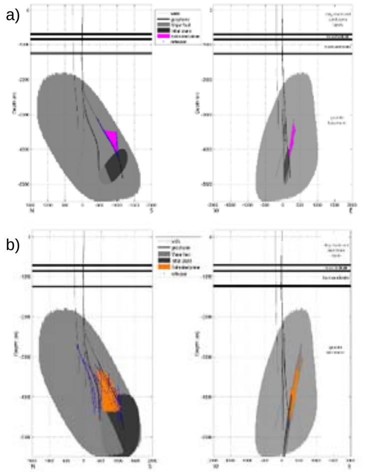

Reflection scheme derived from the modeling for the a) sis2 structure b) sis3 structure, north-south and east-west view.

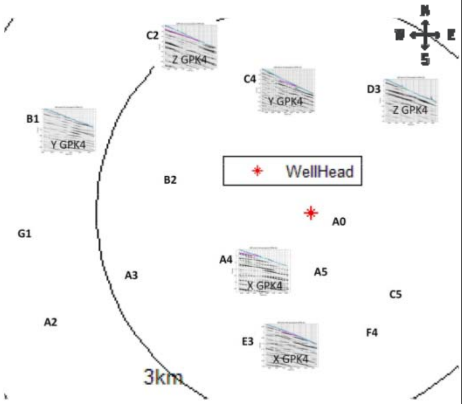

VSP datasets used for SIS2 structure imaging

Lavadera, P. L. (2013).

GFZ Helmholtz Centre POTSDAM

HELMHOLTZ

Acquisition campaign 2007

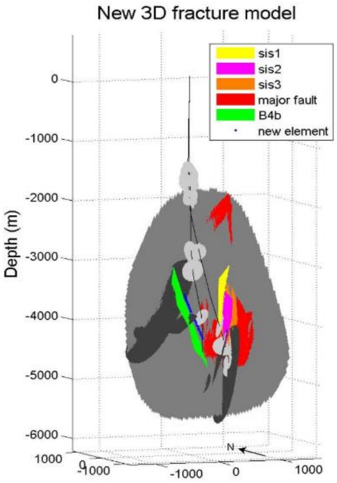

Model defined by Sausse et al. (2010) (black and white) with the resulting structures from VSP (colors).

Lavadera, P. L. (2013).

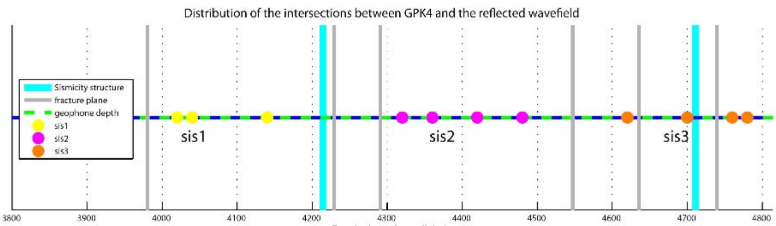

4375-4376 (CAL: increased)
4376 (ABI: cut)
CBL: high amplitude above 4376 (low/no bond)

A major leak was identified from USIT logs in the casing at 4710 MD (4440 TVD).

Lavadera, P. L. (2013).

- The travel time was calculated for reflexions associated with fracture zones.
- Some reflections was explained by structures defined by Sausse et al. (2010) by adjusting their dip and azimuth.
- A new structure which intersects the GPK3 well at 4500 meters was defined.

*This study assumes that the reflections do in PP mode without conversion.

GFZ Helmholtz Centre POTSDAM

HELMHOLTZ

Optimizing the design of vertical seismic profiling (VSP)

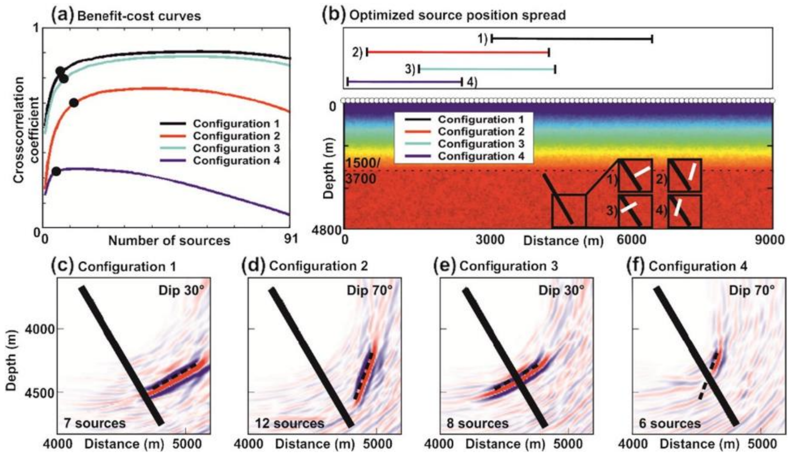

- Borehole maximum inclination 30 °
- 61 receivers placed at 20 m intervals over the depth range of 3700–4900m

(a) Benefit-cost curves for fracture zone configurations 1 to 4 (see Fig. 2). (b) Spread of the optimized source positions for fracture zone configurations 1 to 4 (note that only selected depth segments of the full model (see Fig. 2) are shown, i.e. the depth range between 1500m and 3700m was removed). (c) to (f) Optimized images for fracture zone configurations 1 to 4,respectively.

Reiser, F. et al. (2017).

Optimizing the design of vertical seismic profiling (VSP)

The size of the fracture zone was set to 400m x 400 m x 40 m. Configuration 1 (azimuth 0˚ , represents the ideal setup as in the 2D study) Configuration 2 (azimuth 60˚)

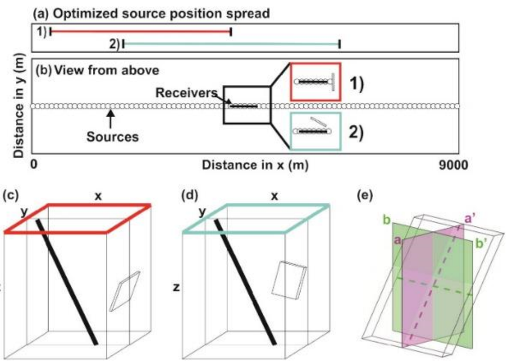

(a) Optimized source position spread for configurations 1) and 2) shown in the conceptual models in (b–d). (e) Two cross sections through the middle of the fracture zone that are used for the 3D optimization.

Reiser, F. et al. (2017).

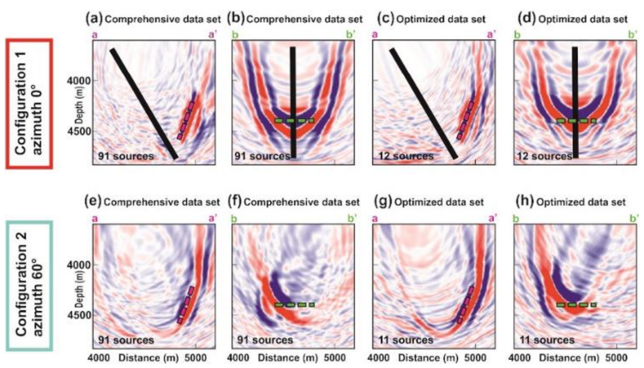

Migrated images for configurations 1) and 2) for the comprehensive dataset and the optimized dataset. The dashed line in magenta represents the length and the dashed line in green the width of the fracture zone.

Reiser, F. et al. (2017).

Suggestions for the planning of DAS VSP survey

Based on the previous knowledge of dip, azimuth and structures extent to plan

- A walkaway VSP survey with optimal source positions for better illumination of the zone of interest. (Reiser, F. et al. 2017) or
- A walkaround VSP (analysis of azimuthal seismic properties) or walkaround VSP with a limited azimuths.

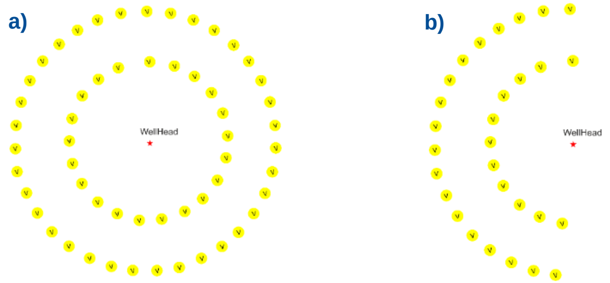

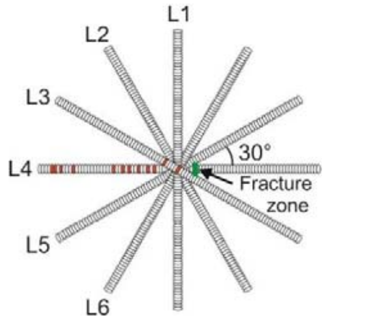

Reiser, F. et al. (2017).

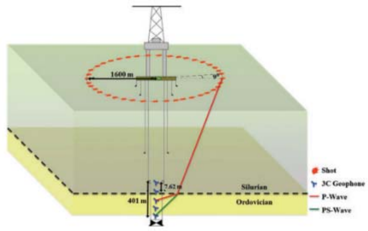

Al Dulaijan, K. et al. (2012).

Careful planning of VSP survey it is required:

- Ray tracing for understanding the illumination of the fault zones
- Modeling for better understanding of expected response

Tube-wave processing and analysis

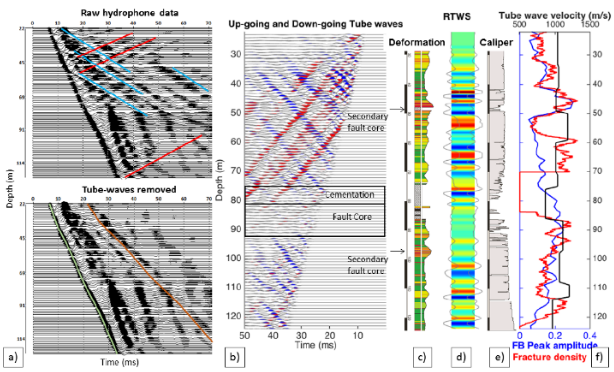

(a) ZVSP data before (top) and after (bottom) up- and down- tube-wave (red and blue lines, respectively) removal through f-k filtering, (b) superposition of up- and down-going tube-waves extracted from the data shown in (a), (c) relative deformation intensity log from core analysis, (d) reflected tube-wave stack (RTWS), (e) calliper log, and (f) first-arrival amplitudes, fracture density from televiewer data and tube-wave velocities. The black box denotes the main fault core and black arrows identify two secondary fault cores.

A. Greenwood, E. et al. (2017).

Seismic processing and imaging

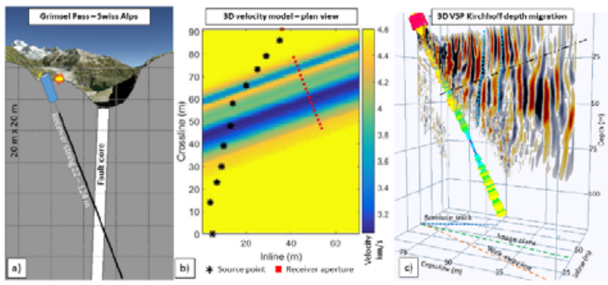

(a) Simplified 2D model of the Grimsel breccia fault, topographic relief, and geometry of the ZVSP survey, (b) plan view of the 3D velocity model derived from smoothed ZVSP interval velocities, surface projection of walk-away sources and extent of hydrophone string, and (c) PSDM image taken on a plane bisecting the borehole plane and walk-away VSP source line. Neutron-neutron data is displayed along the borehole track identifying the main fault core (blue) and upper secondary fault (green), which is bisected by a sub-horizontal structural lineation (dashed black line). Reflections from the top and bottom of the main fault core are indicated by blue dashed lines.

A. Greenwood, E. et al. (2017).

References:

- Baujard, C., Genter, A., Dalmais, E., Maurer, V., Hehn, R., Rosillette, R., … Schmittbuhl, J. (2017). Hydrothermal characterization of wells GRT-1 and GRT-2 in Rittershoffen, France: Implications on the understanding of natural flow systems in the Rhine graben. Geothermics, 65, 255–268
- Al Dulaijan, K., Owusu, J. C., & Weber, D. C. (2012). Azimuthal anisotropy analysis of walkaround vertical seismic profiling vertical seismic profiling: A case study from Saudi Arabia. Geophysical Prospecting, 60(6), 1082–1094.
- A. Greenwood, E. Caspari, J. Hunziker, L. Baron, T. Zahner, D. E. and K. H. (2017). Characterisation and Imaging of a Near-vertical Fault Zone in Crystaline Rock from Hydrophone VSP Data. Fourth EAGE Borehole Geophysics Workshop.
- Lavadera, P. L. (2013). Traitement des donnees de sismique puits acquises en 2007 sur le site de Soultz-sous-Foreets pour la caracterisation de la fracturation du reservoir geothermique.
- Mari, J. & Coppens, F. (2000). Sismique de puits.EditionTechnip, Paris, France: pp240
- Place, J., Diraison, M., Naville, C., Géraud, Y., Schaming, M., & Dezayes, C. (2010). Decoupling of deformation in the Upper Rhine Graben sediments. Seismic reflection and diffraction on 3-component Vertical Seismic Profiling (Soultz-sous-Forêts area). Comptes Rendus Geoscience.
- Place, J., Sausse, J., Marthelot, J.-M., Diraison, M., Géraud, Y., & Naville, C. (2011). 3-D mapping of permeable structures affecting a deep granite basement using isotropic 3C VSP data. Geophysical Journal International, 186(1), 245–263.
- Reiser, F., Schmelzbach, C., Maurer, H., Greenhalgh, S., & Hellwig, O. (2017). Optimizing the design of vertical seismic profiling (VSP) for imaging fracture zones over hardrock basement geothermal environments. Journal of Applied Geophysics, 139, 25–35

GFZ
Helmholtz Centre
POTSDAM

HELMHOLTZ